UNIVERSITÄTSKLINIKUM HAMBURG-EPPENDORF

Klinik und Poliklinik für pädiatrische Hämatologie und Onkologie

Direktor

Professor Dr. rer. nat. Reinhard Schneppenheim

Identifying Molecular Markers for the Sensitive Detection of Residual Atypical Teratoid Rhabdoid-Tumor Cells

Dissertation

zur Erlangung des Grades eines Doktors der Medizin
an der Medizinischen Fakultät der Universität Hamburg

vorgelegt von:

Tu-Lan Vu-Han
aus Wolfsburg

Hamburg 2014

(wird von der Medizinischen Fakultät ausgefüllt)

Angenommen von der Medizinischen Fakultät der Universität Hamburg am:
19.11.2015

Veröffentlicht mit Genehmigung der Medizinischen Fakultät der Universität Hamburg: 03.02.2016

Prüfungsausschuss, der/die Vorsitzende:
Professor Dr. rer. nat. Reinhard Schneppenheim

Prüfungsausschuss, zweite/r Gutachter/in:
Professor Dr. Martin Horstmann

Prüfungsausschuss, dritte/r Gutachter/in:
Professor Dr. Udo Schumacher

Table of Contents

1 Introduction

1.1 The Field of Pediatric Oncology

Sixty-five years ago Sydney Farber discovered one of the first chemotherapeutics Aminopterin, an anti-folate, and successfully applied it against childhood leukemia. Among the many fields of oncology today, the field of pediatric oncology continues to maintain a special position because the long-term effects of successful multimodal treatment will first become evident in pediatric patients. (Devita 1989). Over the years it has "become an axiom that in oncology human cancers often evolve through a multi-stage process that extends over a period of decades. The marked increase in molecular biology studies has revealed that this process is driven by the progressive accumulation of mutations, and epigenetic abnormalities in expression multiple genes that have highly diverse biochemical functions."(Joe 2009). "a significant proportion of central nervous system (CNS) neoplasms affects children: tumors of the nervous system (including retinoblastomas and peripheral neuroblastomas) rank second in incidence after leukemias. In fact, with improvement in the therapy of leukemia, brain tumors are the leading cause of cancer mortality in children. Finally, it is important to point out that they are among the most devastating to patients, since they affect the organ that defines the "self"" (Kleihues 2002).

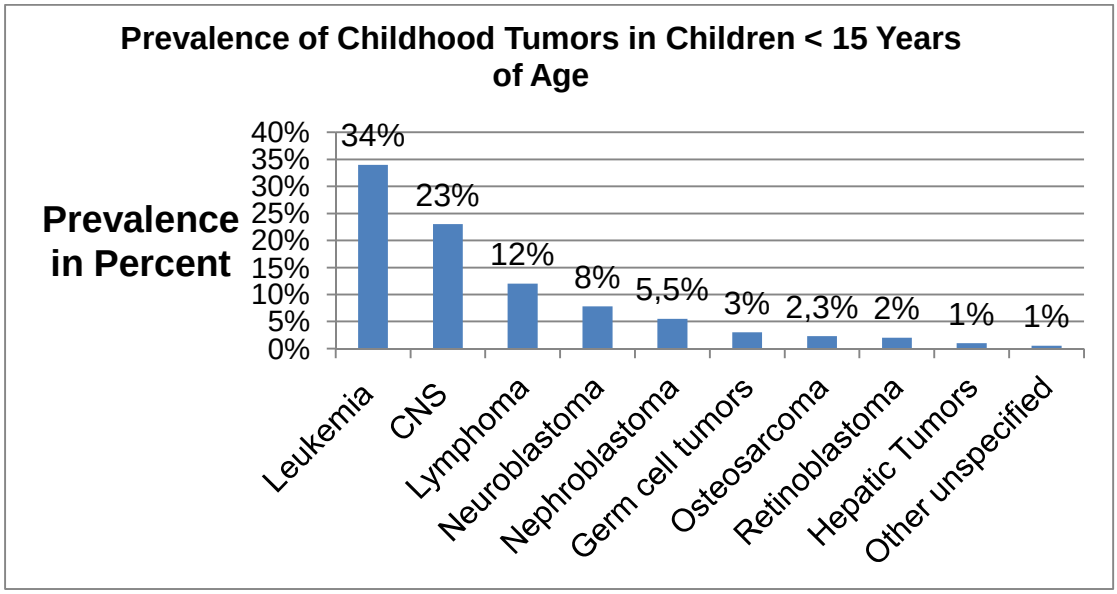

Figure 1 Distribution of Cancer Forms among Children < 15 Years of Age (Kaatsch et al., 2012)

Cancer only makes up approximately 1% of all diseases during childhood; however, it ranks second in causes of death in children below the age of 15 years.

1.2 Atypical Teratoid/Rhabdoid Tumors

1.2.1 Definition and Diagnosis

The atypical teratoid/rhabdoid tumor (AT/RT) is a rare and highly malignant tumor entity of the central nervous system. It was first incorporated in the World Health Organization Classification of Diseases of Oncology (ICDO-3) in 1993 (Kleihues et al. 2002) and first described as a separate entity in 1996 (Rorke et al. 1996). Today AT/RTs are WHO-classified under embryonal tumors 9508/3 and received a WHO-Grade IV, assigning it cytological malignancy, mitotic activity, necrosis-propensity and association with pre- and postoperative disease evolution and fatal outcome (Louis et al. 2007). Its earliest case reports date back to the late 1980's and early 1990's (Ginn and Gajjar 2012). The majority of cases involve patients below 3 years of age and display a male predominance of 3:2 (Rorke et al. 1996). Nevertheless, it must not be neglected that there have been case reports of AT/RT in adults as well (Takahashi 2011 and own unpublished results).

This cancer form is estimated to make up approximately 1-2% of all tumors of the central nervous system during childhood. However, data from institutional reviews and institutional cancer registries encourage the supposition that AT/RT constitutes 50% of all malignant brain tumors in children below the age of one (Packer et al. 2002). The mean age at diagnosis is 17 months (Rorke et al. 1996 and Burger et al. 1998). These tumors occur very rarely in children over six years of age. Even though AT/RT can evolve anywhere in the CNS, it is often found located in the cerebellopontineangle (Rorke et al. 1996) posterior fossa, and supratentorial space (Burger et al. 1998).

This cancer form has frequently been misclassified, due to its close resemblance to the more prevalent childhood tumor medulloblastoma (Burger et al. 1998); ergo its actual number of cases is often considered being underestimated (Chi et al. 2008). AT/RT var-

ies immensely in morphology, which is why many entities must be considered for differential diagnosis, including not only medulloblastoma and primitive neuroectodermal tumors (PNETs) (Chi et al. 2008) but also choroid plexus carcinoma, glioblastoma and germ cell tumors (Bishop and Ali 2012). In fact, AT/RT cannot be distinguished using conventional hematoxylin and eosin (HE) staining. Instead, the diagnosis requires immunhistochemical staining as well as molecular genetic analysis. This circumstance falls in line with the current trend that for many neoplasms, the cytogenetic and molecular genetic profile is increasingly becoming a definitive criterion for classification (Kleihues et al. 2002).

1.2.1.1 Morphology

AT/RT's unique name emerged due to its unusual combination of mixed cellular elements similar to but not typical of teratomas and the rhabdoid cells (Rorke et al. 1996). Rhabdoid cells are characterized by large vesicular nuclei with prominent nucleoli and eccentric cytoplasm with eosinophilic cytoplasmic inclusions (Bishop and Ali 2012). However, in only 10-15% of cases the tumor mass is made up exclusively of classic rhabdoid cells (Louis et al. 2007). The amount of rhabdoid cells can vary greatly, often mixed spindled or pleomorphic undifferentiated cells without a rhabdoid phenotype can be found in the tumor mass, while classic rhabdoid components can remain completely absent (Roberts and Biegel2009). Up to two thirds have components that closely resemble medulloblastoma or extracerebellar PNETs (Kleihues et al. 2002).

1.2.1.2 Immunhistochemical Characteristics

Anti-bodies help distinguish this tumor entity from other primary tumors of the CNS (Rorke et al. 1996). AT/RT is often found to express vimentin, epithelial membrane antigen (EMA), smooth-muscle actin (SMA) and glial fibrillary acidic protein (GFAP)but also in smaller numbers cytokeratins, synaptophysin, chromogranin (Burger et al. 1998), whereas it was usually found to be negative for germ-cell tumor-markers α-fetoprotein, placental alkaline phosphatase and human chorionic gonadotropin (Rorke et al. 1996).

1.2.1.3 Molecular Genetic Analysis

Fluorescence in situ hybridization (FISH) analyses frequently show alterations of chromosome 22. AT/RT was therefore initially associated with monosomy 22 and subsequently deletions and translocations involving chromosome band 22q11 (Roberts and Biegel 2009). Current evidence shows that the gene *SMARCB1*, a tumor suppressor gene located on chromosome band 22q11.2 corresponding with Knudson's two-hit recessive model of oncogenesis, is responsible for AT/RT genesis (Roberts and Biegel 2009). *SMARCB1* consists of 9 exons and spans about 50 kilo base pairs (Versteege et al.1998).The gene encodes for a core member of the chromatin remodeling complex SWI/SNF, responsible for transcription regulation in cells.

1.2.2 Clinical Aspects, Therapy and Prognosis

Clinical Aspects

AT/RT can occur anywhere in the CNS, however, it is often associated with malignant rhabdoid tumors of the kidney (RTK) (Ginn and Gajjar 2012). Furthermore, undifferentiated soft-tissue tumors (Tsuneyoshi et al. 1987) have been described at several different anatomical sites. These tumors were subsequently named extra-renal malignant rhabdoid tumors (ER-MRT). The condition of being predisposed to developing rhabdoid tumors is also known as the rhabdoid tumor predisposition syndrome II (RTPS II, OMIM # 609322). All rhabdoid tumors of different anatomical location share a biallelic inactivation of *SMARCB1* documented in 80% of cases (Sevenet et al. 1999, Biegel et al. 1999, Versteege et al. 1998). *SMARCB1* is a classified tumor suppressor gene responsible for AT/RT genesis; however, there have been reported cases of rhabdoid tumor syndrome where *SMARCB1* was found unaltered (Frühwald 2006). Subsequent discoveries revealed a somatic inactivation of *SMARCA4 /BRG1* gene, confirming that other loci play a role in the genesis of these tumors. The condition in which *SMARCA4/BRG1* is altered is called rhabdoid tumor predisposition syndrome II (RTPS II, OMIM # 613325) (Schneppenheim et al. 2010).

Patients suffering from RTPS show an early-disease-onset, multifocal disease and positive familial cases (Bourdeaut et al. 2011). Metastases through the cerebrospinal fluid are common and found in approximately 20% of the cases at the time of diagnosis

(Tekautz et al. 2005). Metastatic disease is often assessed using a staging system by Chang et al. (1969), in which “M1 is characterized by microscopic tumor cells present in cerebral spinal fluid; M2 indicates nodular seeding demonstrated in the cerebellar, cerebral subarachnoid space, or in the third of lateral ventricles. M3 indicates nodular seeding in the spinal subarachnoid space and M4 indicates extra-CNS seeding” (Dufour et al. 2012, Chang et al. 1969).

Therapy

Due to the early onset of AT/RT, its quick progression and the patients’ young age at the time of diagnosis, the prognosis is often grim. Many physicians hesitate to administer intensive treatment to infants that young age (Bourdeaut et al. 2011) and have previously conducted treatment regimens that were originally designed for other tumors of the CNS, such as medulloblastoma and PNETs (Chi et al. 2008). These therapies have a reported median survival time between 6 and 11 months (Burger et al. 1998, Packer et al. 2002). AT/RT, however, requires a more aggressive multimodal therapy than other brain tumors that is often limited by the therapy’s toxicity to the patient. Hence, the consequences of treatment determine the future direction of therapy (Chi et al. 2008). A total resection of the tumor is one of the primary goals in therapy, however, in practice difficult to achieve without renouncing neurologic functions. Chi et al. (2008) have published the most successful therapeutic strategy against AT/RT to date. The study group tested a treatment divided into five phases: preirradiation, chemoradiation, consolidation, maintenance, and continuation therapy. They were able to achieve higher overall survival rates of 70±10% and event free survival rates of 53±13% with the more aggressive treatment regimen. This regimen consisted of a maximal possible surgical resection of the primary tumor while preserving the neurologic function. An anthracycline based induction therapy was supplemented by intrathecal chemotherapy, using methotrexat, cytarabine and hydrocortisone. An early radiotherapy of 1,8 Gy per fraction and a total dose of 54 Gy was added. Induction therapy was followed by maintenance and continuation therapy with temozolomide and actinomycin-D (Chi et al. 2008).

The rarity of the tumor entity, its quick progression and grim prognosis demands for a standardized registration of epidemiologic, molecular and clinical data of patients with rhabdoid tumors of any anatomical localization. Hence, the European Rhabdoid Regis-

try was founded in 2010. The registry offers consensus therapy recommendations for patients with rhabdoid tumors of the CNS, kidney and soft tissue. These recommendations are based on the data provided by current literature, the investigators' own experience and data from the Society for Pediatric Oncology and Hematology (GPOH) and International Society for Pediatric Oncology (SIOP) studies. The recommendations should be seen as "consented recommendation derived from available data" (Frühwald 2010). The EU-RHAB Study currently recommends a complete, non-mutilating primary resection of the tumor under the microscope, anthracycline based, dose dense regimens, local therapy and early radiotherapy. Intraventricular therapy concomitant or following radiotherapy has been associated with high toxicity and the value of high dose chemotherapy is not yet determined which is why its application is still at the physician's discretion. More details and updates on therapies and schedules should be accessed on the EU-RHAB Study homepage. Further, it must be noted that "the best treatment modality has not yet been established." (Dufour et al. 2012).

Prognosis

Bourdeaut et al. (2011) listed the clinical variables that are thought to influence the prognosis of rhabdoid tumors, which include metastatic disease, complete neurosurgical resection, irradiation, germline mutations and the age at diagnosis. Bourdeaut et al. (2011) discovered that patients with germline-mutations have an overall survival rate of 7,6%, while patients with wild-type germline alleles had an overall survival rate of 29,4% (Bourdeaut et al. 2011). However, considering that germline-mutations are often associated with an early-onset of disease, a Cox regression model that included both age and the presence of germline mutations revealed that age was "the most strongly significant factor" (Bourdeaut et al. 2011). Apparently, available literature is discordant concerning the prognostic factor of germline-mutations. Tekautz et al. (2005) also found age the only statistically significant prognostic factor. Dufour et al. (2012) published a multicenter study conducted in France on clinicopathologic prognostic factors in childhood AT/RT of the CNS, in which the prognostic value of the age (< 2 years) was again confirmed along with the presence of metastatic disease at diagnosis. Furthermore, the study suggested that claudin-6 may be a prognostic factor in AT/RT, as strong positive immunoreactivity was found in 89% of the tumors. Further studies still need to confirm these findings. Dufour et al. (2012) also proposed that endothelial Glucose Transporter

1 be discussed as a possible prognostic factor, as it was found “a useful marker to define the embryonal nature of CNS neoplasms” (Dufour et al. 2012) by Loda et. al (2000).Thus, it can be concluded that the prognosis of AT/RT continues to remain dismal and there is yet a lack of reliable prognostic factors save for the age at diagnosis.

1.3 The Molecular Basis of AT/RT

The molecular basis of AT/RT are homozygous or compound-heterozygous alterations of a gene that the genetic nomenclature committee officially named *SMARCB1* for SWI/SNF Matrix Associated Actin-dependent Regulator of Chromatin Subfamily B Member 1. The gene is also known as IntegraseI nteractor 1 (INI1) or human Sucrose Non-Fermenting gene number 5 (hSNF5). The official name *SMARCB1* will be used in the following. SMARCB1 is a subunit of the SWI/SNF chromatin remodeling complex .The SWI/SNF complex is an evolutionarily conserved multi-subunit chromatin remodeling complex, which uses the energy of ATP hydrolysis to mobilize nucleosomes and remodel chromatin and thereby regulate transcription of target genes (Roberts and Orkin 2004).

1.3.1 Chromatin RemodelingComplex

DNA is present in cells in the tertiary structure form called chromatin. Chromatin's smallest unit is a nucleosome, which consists of 146 base pairs of DNA wrapped 2,5 times around an octamer of histones. The DNA connecting two nucleosomes is called linker DNA, while progressive coiling leads to the compact structure of chromatin. In this condensed form the DNA is not accessible for transcription factors and can only be made accessible either through covalent modification of the histones or DNA, or through a chromatin remodeling complex that mobilizes the histones. Many different variants of the SWI/SNF chromatin remodeling complex exist within mammalians, distinguishable by their lineage-specific subunits (Roberts and Biegel 2009) and dependent on tissue, activation or state, complex type and developmental stage of the cell (Roberts and Biegel 2009). The mammalian chromatin remodeling complex consists of 10-12 subunits including ATPase subunits that utilize ATP to slide the histones along the DNA and thereby selectively expose DNA strands to transcription factors (Cairns et al. 1994, Cote et al. 1994). It has been observed that approximately 5% of all yeast genes are regulated by SWI/SNF at the level of transcription (Sudarsanam et al. 2000, Holstege et al. 1998). However, contrary to primary assumptions that the SWI/SNF complex causes gene up-regulations, it mostly represses them (Roberts and Biegel 2009). An inactivation or loss of function of the SWI/SNF complex core proteins therefore leads to increased transcription, promoting tumor genesis. These findings indeed

provided the first link between chromatin remodeling complexes and tumor suppression (Lee et al. 2013). Various genes, including *SMARCB1, SMARCA4, SMARCA2, PBRM1, ARID1, ARID2, ARID1A, ARID1B,* have since been identified to encode subunits of the SWI/SNF chromatin remodeling complex and linked to different forms of cancer (Lee et al. 2013). Lee and Roberts (2013) even proposed the possibility of "lineage-specific contributions of individual subunits". Cancer genome sequencing studies revealed that at least seven subunits are mutated within the different cancer forms (Wilson et al. 2011). However, *SMARCB1* has been identified to encode a constant and ubiquitous subunit of the SWI/SNF complex, giving it a special position among the various known subunits (Roberts and Biegel 2009).

1.3.1.1 The role of *SMARCB1* in SWI/SNF Complex

The extensive role of SMARCB1 in tumor genesis is widely recognized. However, the actual function of SMARCB1 in the chromatin remodeling complex and the mechanisms that lead to cancer are largely unknown (Wang et al. 2009). Wang et al. (2009) used a mouse model as well as human cells to find that tumor genesis does not result from the absence of SMARCB1. On the contrary, it seems tumor genesis is rather dependent on the presence of SMARCB1, suggesting oncogene addiction, a "phenomenon in which some cancers that contain multiple genetic, epigenetic and chromosomal abnormalities remain dependent on one or a few genes for both maintenance of the malignant phenotype and cell survival" (Joe 2009).

1.3.1.2 Further roles of SWI/SNF chromatin remodeling complex

Besides playing a role in transcription regulation, the SWI/SNF chromatin remodeling complex is also suspected to play a role in DNA synthesis (Flanagan et al. 1999, Lee et al. 1999), viral integration and expression (Kalpana et al. 1994, Yung et al. 2001), mitotic gene regulation (Krebs et al. 2000), and DNA repair causing genomic instability (Klochendler-Yeivin et al. 2006). Although it may seem consequential, how these functions contribute to oncogenesis is yet unclear. Further studies may put light on these matters in the future.

1.4 Molecular Markers for Cancer

Without question the search for molecular markers that predict the presence of cancer and the development of reliable assays that detect them is one of the most promising fields of oncology. The “Identification of predictive biomarkers in circulating tumor cells has the potential to become a breakthrough in cancer diagnostics and drug development.” (Parkinson et al. 2012). Moreover, pediatric brain tumors have distinct pathogenesis and biology, compared with their adult counterparts. Some of the molecular features are so specific to a particular tumor type, such as *SMARCB1* mutations in AT/RT that they could serve as a diagnostic marker on their own (Ichimura et al. 2012). The advantage of circulating tumor markers is their easy obtainment by peripheral blood or alternatively cerebrospinal fluid sampling. The analysis of circulating tumor cells is also termed “liquid biopsy”, which can be repeated on a regular basis, allowing real-time monitoring of metastatic progression (Bednarz-Knoll et al. 2011). Molecular markers could be used on various different levels ranging from diagnosis, detection of metastatic tumor tissue to the monitoring of cancer patients. They could also be prognostic for survival or predictive of response to therapy. Furthermore, molecular markers could be used as indicators in the selection of therapy, in terms of personalized health care and individualized treatment. Molecular profiling of circulating tumor cells could also accelerate drug development and promote targeted therapies against signaling proteins (Parkinson et al. 2012).

The metastatic mechanism of tumor cells is highly complex, as these cells must not only acquire the ability to invade blood vessels but also attain certain mechanisms to survive within the blood stream, which is loaded with immune competent cells that are likely to recognize and lyse the aberrant cells. Metastatic cells must therefore possess the ability to evade these cells and in addition, be able to extravasate and survive in its new environment in order to colonize other sites (Bednarz-Knoll et al. 2011). Once the metastatic cell has found itself a niche, it can establish itself as a secondary tumor mass, undergo apoptosis or remain there over years as an inactive so-called dormant cell (Goss and Chambers 2010). The differentiation between these various states of a tumor cell as well as cell free tumor DNA released by the primary tumor, remains a challenge when developing assays to detect molecular markers for cancer.

1.4.1 The advantages of Mutant DNA as Molecular Markers

The present research objective is to identify specific molecular markers in mutant DNA of AT/RT of the CNS and to determine whether they can be used to detect tumor cells circulating in peripheral blood or cerebrospinal fluid samples. The presence of tumor DNA circulating in plasma or serum of cancer patients was first demonstrated in 1977 (Leon et al. 1977). The main advantages of using mutant DNA as biomarkers are for one, its availability, as mentioned above, but also its stability, since mutant DNA appears to be stable for several years when stored in samples of plasma or serum. Furthermore, its relative simplicity of use, by extracting it using conventional purification methods is highly convenient in clinicopathological practice (Gormally et al. 2007). Gormally et al. (2007) also contrasted its disadvantages, the lack of specificity, as they are not indicative of tumor type and site and further the possibility that altered DNA is present in healthy subjects for various unknown reasons. However, these disadvantages mentioned by Gormally et al. (2007) do not apply for this research objective, as these molecular markers will be highly specific for each individual patient. They do not need to be indicative of tumor type, because the tumor type will already have been determined prior to monitoring and residual cell detection, respectively.

1.5 DNA-Repair Mechanisms

Genetic diversity is indispensable for the permanent survival of a species, because it benefits the evolution of a species to adjust to an ever changing environment (Alberts et al. 2008). Genetic changes within the genome are therefore promoted by tightly regulated physiological processes, such as meiosis and immune repertoire generation (Grabarz et al. 2012). Even the genome itself is laid out to promote genetic diversity, i.e. through transposable elements that have the intrinsic ability to change their position within the genome naturally causing genetic alterations. Ionizing radiation, metabolism, substances in the environment and chemotherapeutic drugs also generate alterations in the genome. Thus, DNA in living organisms is constantly exposed to both external and internal mutagens, incurring countless types of damages (Friedberg 2003). Genetic changes within the individual, however, can be pathogenic or even fatal. The maintenance of the balance between preserving genetic stability and promoting genetic diversity requires tightly regulated processes (Grabarz et al. 2012).

A central process within maintaining that equilibrium is DNA-repair. Various pathways using different enzymes exist to repair different types of damages in the DNA. An especially delicate lesion is the potentially cytotoxic double-strand DNA break (DSB) (Karanam et al. 2012).Two distinct pathways are known to repair DSBs, non-homologous end joining (NHEJ) and homologous recombination (HR), while a third is being discussed in recent literature called alternative end joining (A-EJ) (Grabarz et al. 2012). Defects in these pathways have been associated with immunodeficiency, cancer predisposition and other diseases (Karanam et al. 2012).

1.5.1 Non-homologous End Joining

Non-homologous end joining is the dominating DSB repair pathway in humans (Lieber et al. 2003). In fact, Karanam et al. (2012) demonstrated in quantitative live cell imaging that NHEJ is the dominant repair mechanism during G1- and G2-phases of the cell cycle, while the highest activation of homologous recombination is reached in mid S-phase. These findings also confirmed the previous postulations that the pathway chosen is dependent on cell cycle. NHEJ underlies an overall simple mechanism: the two ends of double-stranded DNA are aligned, processed and ligated. NHEJ has a tendency for

microhomology usage, i.e. the two ends are joined with higher efficiency when 1-4 nucleotides are complementary between the two ends (Roth and Wilson 1986). Microhomology is not always given; in these cases NHEJ is highly erroneous as it goes along with the loss of nucleotides (Lieber et al. 2003).

1.5.2 Homologous Recombination

Homologous recombination (HR) is the more accurate DSB repair pathway. It is initiated by single stranded DNA (ssDNA) resection and subsequent invasion of a homologous double-stranded DNA (dsDNA) leading to strand exchange. This process requires a minimal length of perfect homology between the two strands. In mammalian cells the length of this so-called Minimal Efficient Processing Segment (MEPS) ranges from 200 to 250 bp (Liskay et al. 1987, Lopez et al. 1992, Rubnitz and Subramani 1984). A new dsDNA molecule called heteroduplex is the result of the strand exchange. Missing nucleotides are filled in by DNA polymerases. HR usually enables a flawless repair of DSBs.

1.5.3 Alternative End Joining

A third and rather poorly characterized DSB repair pathway is the alternative end joining (A-EJ), also known as Backup-NHEJ (B-NHEJ) or Micro-Homology Mediated End Joining (MMEJ) (Grabarz et al. 2012). A-EJ is described as highly mutagenic; it is associated with deletions at the junctions and is discussed as a major source of DNA translocations induced by DSB (Boboila et al. 2010, Guirouilh-Barbat et al. 2004, Simsek and Jasin 2010, Weinstock 2007). A-EJ is, like HR, also initiated through ssDNA resection, however, it requires no extended resection or extended sequence homology and is independent of various enzymes such as Ku80 and XRCC4, distinguishing it from NHEJ. A-EJ is a pathway that should be repressed, regulation processes are required to avoid the A-EJ pathway once the first initiation step (resection) has been made for HR.

Lieber et al. (2003) discussed reasons for NHEJ being the predominant pathway, despite its high error rate. They concluded that 40% of the human genome is repetitive and HR in a repetitive portion of the genome is therefore probabilistic and profound genomic

rearrangements could be the consequence (Grabarz et al. 2012). Furthermore, HR requires sequence homology and the donor is required to be directly adjacent, which is only the case during late S- and G2-phases.

1.6 Research Objective

The gene *SMARCB1* is located on chromosome band 22q11.2. This region seems to underlie a certain genetic liability for double-stranded DNA breaks (Lee and Roberts 2013) and various other genetic mutations. The most common germline mutations have been found to be point or frameshift mutations that lead to a premature truncation of the protein. Intragenic deletions are likewise distributed among both somatic abnormalities as well as germline. They can involve 1 exon to all 9 exons of *SMARCB1*, however most preferentially exons 4 and 5 are mutated (Eaton et al., 2011). The mutations in AT/RT tumor tissue have thus been characterized. However, the deletions and their according breakpoints have not yet been examined extensively. The first objective is therefore to identify breakpoints in AT/RT patients and to map and characterize them for future understanding of this region.

Contemporary cure for cancer consists of early detection, multimodal treatment and again early detection by closely monitoring the patients. Therefore, there is much effort being put into the discovery of methods that could sensitively predict the presence of cancer. This research objective, too, aims at identifying possible molecular markers for this purpose. The idea of mutant DNA from the bloodstream being used as molecular markers for cancer is not a novel idea. Detecting mutant DNA in the blood stream is a method that has been successfully established for the Minimal Residual Disease (MRD) in acute lymphatic leukemia (ALL) and is on the verge of being established for a series of other tumor types. The identified genetic alterations in the tumor are highly heterogeneous and therefore specific for each patient. For the purpose of individualized treatment, the patient's tumor specific mutations could be used to detect residual cells in peripheral blood or cerebrospinal fluid samples, in the sense of molecular markers. The detection method in this research objective uses specific primers to the mutation site and real-time-PCR for quantification. The following research objective is to serve as a proof-of-principle. Future research objectives can then establish standardized methods on the ground of these findings and perhaps one day introduce them to clinical pathology. Early detection followed by early therapy has beneficial influence on the prognosis of cancer patients. The unfavorable prognosis of these cancer patients underlines the

importance of a sensitive monitoring technique and even demands them in order to enhance the chances of survival for AT/RT patients.

2 Material and Methods

A detailed description of all the instruments and materials used are listed in the appendix. All methods used were adjusted for the individual circumstances of each patient's unique material provided. Each patient was characterized by unique limitations in either quality or quantity of DNA provided and unique genetic alterations within the tumor.

2.1 Patient-Sample Selection

The atypical teratoid rhabdoid-tumor is a rare tumor entity. The Department for Pediatric Hematology and Oncology Hamburg-Eppendorf serves as a reference laboratory for diagnostics of the EU-Rhab Register and therefore possesses an extensive collection of tumor-material from all over Europe. Out of a contingent of approximately 150 patients a total of seven patients were selected from the database for proof-of-principle. The first selection criterion was a molecular genetically ascertained diagnosis of AT/RT with alterations on the *SMARCB1*-Gene of both alleles. For a sensitive detection of residual tumor cells in periphery blood of the patient, an additional requirement was that all patients with germline mutations must be excluded, as patients with germline mutations would show the identified mutation in all of their cells and a specific detection of residual tumor cells would therefore not be possible. The tumor material was provided either by the pathology department of the University Hospital Münster where the tumor was formalin fixed, embedded in paraffin and stored, or by the Department for Pediatric Hematology and Oncology of the University Clinic Hamburg-Eppendorf.

A consent form for the application of patient material for research purposes is available for every patient. As part of the EU-Rhab Register this scientific study was covered by approval of the ethics committee.

2.2 DNA Extraction

The experiments required genomic DNA from tumor tissue and peripheral blood of the patients. DNA from fresh frozen tumor tissue and peripheral EDTA – blood from Patient 1 and 7 was extracted using the QIAmpDNA Mini Kit for Tissue & Blood by Qiagen. Extracted DNA from patients two to six was provided by the Pathology Department of the University Hospital Münster.

2.3 Breakpoint Localization

2.3.1 Multiplex-Ligand-dependent Probe Amplification (MLPA)

Multiplex PCR is a deletion- screening technique first successfully established by Chamberlain JS et al. (1988) for Duchenne muscular dystrophy. Multiplex-Ligand-dependent Probe Amplification (MLPA) by MCR-Holland is a method based on the idea that multiple amplifications on the same template DNA can provide information concerning deletions on the template. MRC-Holland provides kits that allow a copy number determination of up to 50 DNA sequences in a single multiplex PCR-based reaction. The method is sensitive enough to detect gene dosage reduction on one allele or both, respectively. In order to roughly characterize heterogeneous changes on chromosome 22 the SALSA MLPA Kit P258 *SMARCB1* and SALSA MLPA Kit P250 DiGeorge were used. Both Kits are suitable for the analysis of Chromosome 22, with the benefit that DiGeorge covers a larger region beyond that of *SMARCB1*. By combining the results from both kits, the distribution of molecular genetic deletions could be roughly localized. The breakpoint regions were also narrowed down to a few hundred thousand or million base pairs, respectively.

2.3.2 Primer Design

The published FASTA-formatted sequence of Chromosome 22, NCBI Reference Sequence NT_011520.12 (NCBI Nucleotide Database) was loaded onto Lasergene 8 SeqBuilder Programme by DNAstar. The program allows DNA sequence alteration and markings on the sequence, as well as primer design. The program was also used to keep an overview of all the primers used along the sequence. PCR primers for primer walking on the ThermoCycler were designed with melting temperatures (T_m) at 71°C ± 2°C.

PCR primers for the LightCycler Instrument were designed with T_m at 60°C ± 1°C. The primer T_m was determined using Metabion International AG's Biocalculator.

The length of the primer products was held between 120-300 base pairs, depending on the quality of the material used. Qiagen generally recommends aiming for shorter primer product sequences when working with FFPE material (ideally 120 ± 50 base pairs). Nevertheless, Qiagen also reported of successful molecular genetic analysis using up to 300 base pairs (Unlocking your FFPE Archive, Sample and Assay Technologies by Qiagen FFPE Brochure 09/2010).

2.3.3 Primer Walking PCR

After having roughly localized the breakpoints via MLPA, primer pairs flanking the supposed breakpoint region were placed using the published sequence of Chromosome 22. A PCR-Reaction using GoTaq Green Master Mix by Promega was prepared according to protocol. The specificity of the primer pairs were tested using wild type DNA prior to analyzing the tumor tissue. The reaction mix contained 25 µl GoTaqGreen MasterMix, 20 µl H_2O + 2 µl $MgCl_2$ + 1 µl of 100 mM forward primer + 1 µl of 100 mM reverse primer + 1 µl of 1-5 ng/µl DNA. The primers had annealing temperatures of 68°C to ensure high specificity. Occasionally a primer pair would improve PCR efficiency at an annealing temperature of 65°C. The ThermoCycler was programmed accordingly:

Table 1 Block Cycler Program for PCR

	Step	Temperature	Time	
1	Preheating	95 °C	∞	
2	Initial denaturation	95 °C	5 Min.	
3	Denaturation	95 °C	30 s	
4	Annealing	65/68 °C	30 s	
5	Extension	72 °C	30 s	go to 3 x 35
6	Final extension	72 °C	5 Min.	
7	Cooling	15 °C	∞	

Primer pairs placed within a deleted region of the tumor sequence did not amplify, which was discernable by the lack of a band in the agarose gel electrophoresis. Template without deletion by contrast would deliver a band in agarose gel electrophoresis,

serving as a positive control. By comparing the two bands and subsequently placing additional primer pairs within the supposed breakpoint region, the breakpoint was limited down to 200-500 base pairs.

2.3.4 Deletion Spanning PCR

Once the breakpoint region was limited down to 200 or 500 base pairs, the flanking primer pairs were used for deletion spanning PCR. It was uncertain how large the actual product would be, because it was unclear whether a large deletion or several smaller non-consecutive deletions existed within the supposed breakpoint region.

DreamTaq DNA Polymerase is an enhanced Taq DNA Polymerase that is capable of producing longer PCR products and higher yields compared to conventional Taq DNA polymerase. Deletion spanning PCR was most successful using DreamTaq PCR Master Mix (2X) by Thermo Scientific.

Deletion spanning PCR was graded successful, when the agarose gel analysis revealed one distinct band in the tumor tissue while none to be found in the wild type controls (see also Figures in the Result section). The agarose gel band was cut out, sequenced and subsequently analyzed with a Basic Local Alignment Search Tool, BLAST-Program. The program analyzes and compares the query nucleotide sequence with sequence databases and calculates the statistical significance of matches. It is useful when searching for unknown sequences. The results of a BLAST-Search delivered the exact breakpoint. After having inserted these results, the magnitude of the deletion was calculated with help of the reference sequence loaded into Lasergene 8 SeqBuilder Program.

If the deletion spanning PCR-product was expected to be larger than six thousand base pairs, which was the case when a breakpoint could not be narrowed down further due to poor material quality or heterogeneous deletion, an alternative kit was used for deletion spanning PCR. The deletion spanning PCR usedLongRangeDNTPack by Roche Applied Sciences. The kit is said to have been optimized for the amplification of large fragments of 5 kilo bases to 25 kilo bases pairs with a threefold higher fidelity than Taq DNA polymerase. A PCR vessel for the tumor template DNA ran along with five dif-

ferent wild-type controls, in order to exclude amplifications of random sequences that occur commonly in specific populations.

The Long Range dNTPack reaction mix contained 31,3 µl H_2O + 10 µl Long Range Buffer with $MgCl_2$ + 2,5 µl Nucleotide Mix + 1,5 µl Forward primer + 1,5 µl reverse primer + 1,5 µl DMSO (or H_2O depending on the region) + 0,7 Polymerase and 1 µl DNA.

The Block Cycler was programmed accordingly:

Table 2 Block Cycler Program for Expand Long Range PCR

	Step	Temp.	Time	Cycles
1	Denaturation	92 °C	2 Min.	1x
2	Denaturation	92 °C	10 s	10 x
3	Annealing	65 °C	15 s	
4	Elongation	68 °C	10 Min.	
5	Denaturation	92 °C	10 s	25x
6	Annealing	65 °C	15 s	
7	Elongation	68 °C	10 Min. + 20 s cycle elongation for each succesive cycle	
8	Final Elongation	68 °C	7 Min.	1x
9	Cooling	8 °C	∞	

2.4 Agarose Gel Electrophoresis and PCR product Extraction

All PCR-products were separated using a 1,2% agarose gel electrophoresis made up of 1,2 g agarose+ 100 ml TAE Buffer. Deletion spanning PCR-products were cut out using a sharp scalpel on a UV-Lighttable. The PCR product was extracted from the gel using QIAquick Gel Extraction Kit by Qiagen according to protocol.

2.5 Sequencing

PCR-products were sequenced on an ABI-Prism 3130 Genetic Analyzer using the ABI Prism BIG DYE Terminator Cycle Kit. Sequencing reaction vessels contained 13 µl H_2O + 1,5 µl Primer (forward or reverse) + 0,5 µl BIG DYE + 3,5 µl HT Buffer. The PCR pre-going sequencing on the ABI-Prism 3130 Genetic Analyzer was programmed according to Table 3 Block Cycler Program for Sequencing:

Table 3 Block Cycler Program for Sequencing

	Step	Temperature	Time	Number of Cycles
1	Preheating	95 °C	∞	
2	Initial Denaturation	95 °C	5 Min.	
3	Denaturation	95 °C	30 Sek.	
4	Annealing	variable (Primer Tm)	30 Sek.	
5	Elongation	60 °C	4 Min.	go to Step 3 x 80
6	Cooling	15 °C	∞	

In case of Patient 2 the quantity and quality of the DNA was expected to be reduced, due to formalin fixation and paraffin embedding. Therefore, a higher amount of template DNA was applied for sequencing reaction mix. It contained 4 µl DNA + 1,5 µl Primers (forward or reverse) + 1,5 µl BIG DYE + 3 µl HT Buffer + 10 µl H_2O. The same block cycler program was used as shown in Table 3 Block Cycler Program for Sequencing.

2.6 Fragment Analysis

Homozygous deletions on both alleles, as discovered in patient 2, can indicate that both alleles have been knocked out by two events. One probable mechanism is a uniparental isodisomy, when both homologous chromosomes derive from the same parent. In order to understand the mechanism behind the singular mutation more thoroughly, a fragment analysis was done. Fragment analysis used a total of sixteen 5'-FAM-marked primer pairs for single nucleotide polymorphisms (SNPs) distributed across chromosome 22, flanking the *SMARCB1*-region. The reaction mix contained 38,3 µl H_2O + 5 µl 10x PCR Mix + 2,5 µl $MgCl_2$ + 1 µl dNTPs + 2 l Primer Mix + 0,2 µl Taq Polymerase + 1 µl DNA (3 ng/µl). The block cycler was programmed according to table 4.

Table 4 Block Cycler Program for Fragment Analysis

	Step	Temperature	Time	Number of Cycles
1	Preheating	95 °C	∞	
2	Initial Denaturation	95 °C	5 Minutes	
3	Denaturation	95 °C	30 Seconds	
4	Annealing	56-68 °C (Gradient)	30 Seconds	
5	Elongation	72 °C	30 Seconds	go to Step 3 x 25
6	Final Elongation	72 °C	20 Minutes	
7	Cooling	15 °C	∞	

After amplification on the BlockCycler, the amplified fragments were analyzed on the ABI-Prism 3130 Genetic Analyzer. Each reaction vessel contained 2 µl of the PCR reaction product + 0,25 µl Gene Scan 500 LIZ + 17,75 µl Formamide.

2.7 Real-Time PCR

One of the latest technologies for nucleotide quantification is real-time PCR. The method uses fluorescent dyes that are excited at a certain wavelength; the emission signal is subsequently detected by the instrument. There are a number of different fluorescent dyes and detection methods on the market. Two different fluorescent dye detection methods have been used for residual AT/RT cell quantitative detection: SYBR Green I and the TaqMan-principle using a dual-marked probe (Mühlhardt 2009).

Real-time PCR uses the kinetics of the PCR-reaction to quantify the nucleotides. The amplification of the template can be subdivided into a baseline, exponential and plateau phase (see also Figure 2 Characteristic curves in real-time-PCR). During the baseline phase the fluorescent signal of amplification is yet below the detection limit, it is followed by an exponential phase during which the fluorescence correlates with the amount of amplification. During the plateau phase, the amplification begins to cease due to substrate depletion and feedback-inhibition through the accumulation of end products, such as pyrophosphates. For quantification the formerly so called threshold cycle (Ct), or more recently known as cycle of quantification (Cq) is used. Cq is the cycle, during which the curve cuts the baseline and the exponential phase begins.

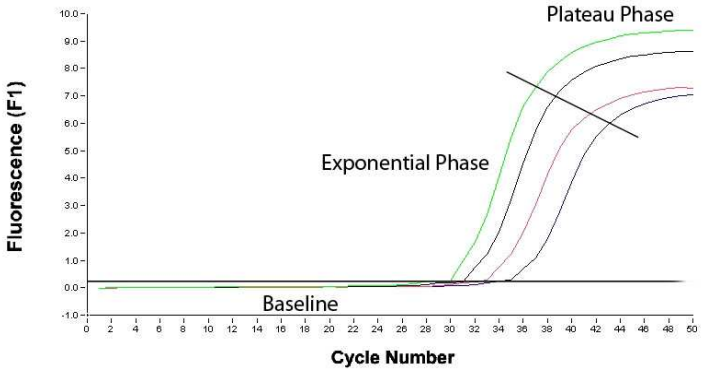

Figure 2 Characteristic curves in real-time-PCR

Low concentration of target DNA used to be a concern, due to unspecific amplifications. Modern hot start methods, also used in Quantifast SYBR Green I PCR by Qiagen and FastStart DNA MasterPlusHyprobe PCR by Roche Applied Sciences, have eliminated this concern. The primer specificity can be further tested via melting curve analysis. This analysis method usually takes place at the end of amplification. The temperature is continuously increased from 40°C to 95°C. The PCR products are increasingly melted by the rising temperature. Assuming that unspecific primer products will vary in product length and larger products will melt at a higher temperature than short products, the fluorescent signal will peak accordingly at a certain temperature. Ideally, there should be only one distinct peak in the melting curve if the primer product is specific (see Figure 3 real-time PCR: Melting Curve Analysis).

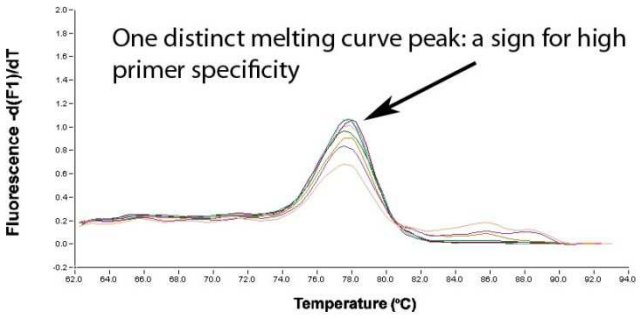

Figure 3 real-time PCR: Melting Curve Analysis

Real-time PCR is generally highly sensitive and therefore liable to minimal differences in starting concentrations. Careful adjustments in starting template with DNA specific measuring tool, such as Qubit Fluorometer 2.0 by Life Technologies, are therefore necessary for successful real-time PCR.

2.7.1 Quantifast SYBR Green I for residual AT/RT Cell Detection

Quantifast SYBR Green I (Molecular Probes) is one of the most common fluorescent dyes in real-time PCR. It intercalates with double-stranded DNA, absorbs blue light at a wavelength of 494 nm and emits a green light at a wavelength of 521 nm. Its main advantages are its versatility, high signal strength and low signal-background-ratio. Accordingly, its disadvantage is the high amount of artifacts produced in a LightCycler Amplification run.

Once the breakpoint sequence was identified in the tumor tissue, mutation-specific primers were designed for residual tumor cell detection. Once the fluorescent chrome attached itself to double-stranded DNA the fluorescent signal would be detected by LightCycler Instrument, causing the characteristic curves on the screen. This method works well for quantification purposes as described above, as well as for residual tumor cell detection. The amount of DNA used ranged between 1-5 ng in 20 µl reaction vessel, most experiments proving best detectability when applying DNA-concentrations < 50 ng/µl. The specificity was analyzed by performing melting curve analysis.

2.7.2 Quantifast SYBR Green I for Gene Dosage Quantification

SYBR Green I, as stated above, is universally applicable for real-time PCR. A further application of the same Quantifast SYBR Green I kit by Qiagen was a relative gene dosage quantification using a housekeeping gene.

Relative quantification is based on the change in threshold cycle calculated with help of the $2^{-\Delta\Delta Ct}$ - Method (Livak and Schmitgen 2001). The quantification enabled a distinction between deletions on one or both alleles. Heterozygous breakpoint regions, as were found in Patient 1, could only be narrowed down by gene dosage quantification. The experiments proceeded on the assumption that a deletion on one allele, would quantify

as fifty-percent gene dosage, while a deletion on both alleles would quantify as zero percent gene dosage and no deletion on either allele would quantify as 100-percent gene dosage, respectively. The same procedure for primer walking was followed as described above when using conventional PCR. The kit was used according to protocol. The reaction vessels contained 10 µl SYBR Green MasterMix + 1,6 µl HPLC-purified Primer Mix (forward and reverse) + 7,4 µl H_2O + 1 µl DNA Template (3-5 ng/µl). At least two different wild type DNAs served as positive controls. The amount of template DNA was carefully adjusted using Qubit Fluorometer 2.0 dsDNA broad range. Conventional DNA concentration measurement via photometers is rather unspecific and not sufficiently precise for real-time PCRs.

Table 5 Light Cycler Program for Quantifast SYBR Green PCR Kit

	Step	Temperature	Incubation	Temp. Transition C°/s	Acquisition mode
1	Initial activation	95 °C	05:00	20	NONE
2	PCR Cycling	95 °C	10	20	NONE
3		60 °C	30	20	Single
4	Melting Curve	95 °C	15	20	NONE
5		60 °C	15	20	NONE
6		95 °C	0	0,1	Continuous
7	Cooling	40 °C	30	20	NONE

The Light Cycler instrument was programmed as described above in Table 5 Light Cycler Program for Quantifast SYBR Green PCR Kit.

2.7.2.1 Comparative Quantification

The nucleotides were quantified using a relative quantification method called $2^{-\Delta\Delta Ct}$-Method. Comparative quantification distinguishes the heterozygous deleted regions from the non-mutated regions through examination of the crossing point values. This required a formula using the spreadsheet program Microsoft Office Excel, each run could be calculated and compared to a reference gene (here: CFTR-Gene Exon 4, under

the presumption that chromosome 7 is unaltered in all patients). Each LightCycler run required at least duplicate reaction vessels in order to opt out pipetting errors. Roche recommends a Fit Points Analysis for SYBR Green PCR, through which the baseline can be adjusted manually. The baseline adjustment cancels out background and noise. Once the cycle of quantification Cq could be read off the screen, calculations could begin. Ct-values of duplicate vessels may not differ more than ≥ 0,5.

The following steps were followed to create a uniform sample sheet used for all of the experiments.

Table 6 Template for Cq-Value Transfer

		A	B	C	D	E
	Ct-Values	Primer # 1	Primer # 2	Primer # 3	Primer # 4	Ref-Gene
1	Patient					
2	Patient					
3	C1					
4	C1					
5	C2					
6	C2					

C1 = Control 1, C2 = Control 2

Step 1 – Arithmetic Mean Value Calculation

In the first calculation step the arithmetic mean value of the duplicate reaction vessels are calculated.

$$M_{ct} = \frac{1}{n}\sum Ct_i = \frac{Ct_1 + Ct_2 + \cdots Ct_n}{n}$$

M_{ct}= arithmetic mean value of crossing point values of identical reaction vessels
n = the number of identical reaction vessels in one LightCycler run
Ct=crossing point values for each of the identical reaction vessel received through Fit Point Analysis

Table 7 Template for Mean Value Calculation

		A	B	C	D	E
	1. Mean Values	# 1	#2	#3	# 4	Ref-Gene
7	M Patient	(A1+A2)/2	(B1+B2)/2	(C1+C2)/2	(D1+D2)/2	(E1+E2)/2
8	M C1	(A3+A4)/2	(B3+B4)/2	(C3+C4)/2	(D3+D4)/2	(E3+E4)/2
9	M C2	(A5+A6)/2	(B5+B6)/2	(C5+C6)/2	(D5+D6)/2	(E5+E6)/2

This calculation step is done for the patient, control 1, control 2 and every primer pair including the reference-gene primers.

Step 2 – Calculating the Difference to the Reference Gene

In a second step the difference between the mean value and the mean value of the reference gene is calculated. The reference gene serves as an internal control. Amplification differences due to differences in material quality are eliminated through this step.

$$\Delta Ct = M_{ct-primer\#} - M_{Ref}$$

Table 8 Template for Calculating the Difference to Reference Gene

		A	B	C	D	E
	2. Differences	# 1	# 2	# 3	# 4	Ref-Gene
10	Pat Mct-MRef	A7-E7	B7-E7	C7-E7	D7-E7	E7-E7 = 0
11	C1 Mct-MRef	A8-E8	B8-E8	C8-E8	D8-E8	E8-E8 = 0
12	C2 Mct-MRef	A9-E9	B9-E9	C9-E9	D9-E9	E9-E9 = 0

Step 3 – Calibration

In the third step, the wild type controls are defined as 100% gene dosage, in order to calculate the patient samples in relation to the wild type.

$$\Delta\Delta Ct = \Delta Ct - \Delta Ct_{calibrator}$$

$\Delta Ct_{\text{calibrator}}$= the difference of wild type sample to reference gene.

Table 9 Calibration Template

		A	B	C	D	E
	3. Calibration	# 1	# 2	# 3	# 4	Ref-Gene
13	Patient	A10-A11	B10-B11	C10-C11	D10-D11	E10-E11
14	C1	A11-A11	B11-B11	C11-C11	D11-D11	E11-E11
15	C2	A12-A11	B12-B11	C12-C11	D12-D12	E12-E11

Step 4 – Converting $\Delta\Delta Ct$ into Absolute Values

The fourth step uses a formula in order to convert the values into absolute numbers that can be compared to one another.

$$Genedosis = 2^{-\Delta\Delta CT}$$

Table 10 Conversion Template

		A	B	C	D	E
	4. Conversion	# 1	# 2	# 3	# 4	Ref-Gene
16	Patient	2^(-A13)	2^(-B13)	2^(-C13)	2^(-D13)	2^(-E13)
17	C1	2^(-A14)	2^(-B14)	2^(-C14)	2^(-D14)	2^(-E14)
18	C2	2^(-A15)	2^(-B15)	2^(-C15)	2^(-D15)	2^(-E15)

A graphic demonstration of the results from step four can show differences in gene dosage.

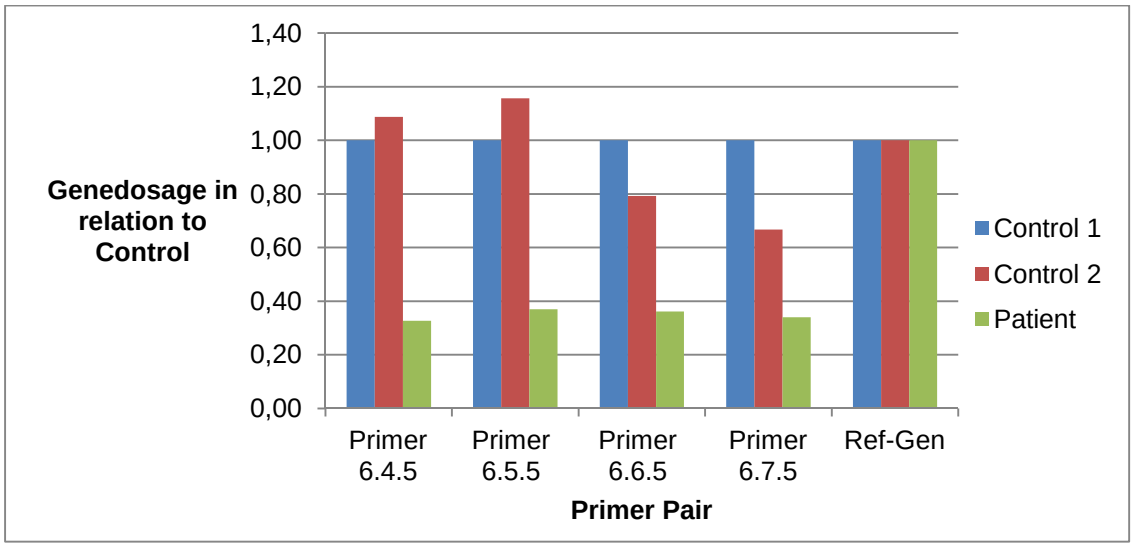

Figure 4 Tumor Gene Dosage in Relation to Wild type Control

Figure 4 Tumor Gene Dosage in Relation to Wild type Control demonstrates what a graphic demonstration of the $\Delta\Delta CT$ – values can look like. The patient's tumor tissue shows decreased gene dosage compared to wild type, indicating that the primer pairs used lie within the heterozygous deleted region.

2.7.3 The TaqMan Principle real-time PCR

The poor specificity of the fluorescent dye SYBR Green I can be circumvented using a third oligonucleotide that is designed to bind between the forward and reverse primer. This oligonucleotide has a 5' 6-FAM (Reporter) and 3' BHQ-1 (Quencher) labeling. Once the taq-polymerase releases the oligonucleotide using its 5'-3'-exonuclease-activity the signal strength increases (Mühlhardt 2009). This so called TaqMan principle is the oldest (Livak et al. 1995) and probably most common technique in real-time-PCR.

FastStart DNA MasterPlusHyprobe by Roche Applied Sciences. The PCR primer pairs were designed to be specific for the tumor's mutation site. The specificity was tested with SYBR Green I, as described above. For additional specificity a 5' 6-FAM – 3' BHQ-1–marked probe was designed between the forward and the reverse primers. 6-FAM is the fluorescent marker that is excited at a wavelength of 488 nm and emits fluorescent signal at a wavelength of 518 nm. BHQ-1, a BlackHole Quencher that covers wavelengths of 500-580 nm, (TIB MOLBIOL Synthese labor GmbH 2009) will decrease the fluorescence of 6-FAM when in close proximity to it.

Table 11 Light Cycler Program for FastStart DNA MasterPlusHyprobe

		Temp.	Time	Transition Rate C°/s	Acquisition mode	Number of Cycle
1	Pre-Incubation	95 °C	10 Min.	20	None	
2	Amplification	95 °C	15 s	20	None	
3		60 °C	15 s	20	Single	
4		72 °C	15 s	20	None	go to step 2 x 45
5	Cooling	40 °C	30 s	20	None	

The Light Cycler was programmed as described in Table 11 Light Cycler Program for FastStart DNA MasterPlusHyprobe.

2.8 Calculation steps for Residual Tumor Cell Detection Limit

The concentration of extracted DNA from tumor material determined the initial concentration of each dilution series. One 100% tumor cell DNA vessel and a 100% normal cell vessel with the same starting concentration were placed in each run. The initial concentration without dilution in a normal cell DNA background was defined as 100% tumor cells. The lowest concentration of tumor cell DNA in a background of normal cell DNA that still amplified during the tumor cell search real-time PCR was determined as the detection limit.

3 Results

Each of the seven patients revealed highly heterogeneous and unique mutation sites in the tumor. Quality and quantity of tissue and DNA used were also highly heterogeneous, which is why, an individual depiction of results for each patient has been decided upon. Every patient's tumor posed different challenges, requiring different dilution series, initial concentrations and methods to attain the research objective. There is not yet a standardized method, though future objectives could develop one on the grounds of these ergonomic findings. All patients are treated anonymously and will be referred to as male.

3.1 Patient 1

Patient 1 first displayed symptoms at the age of 24 month. Molecular genetic analysis revealed two different very large deletions on both alleles in the tumor.

3.1.1 Patient 1 MLPA Results

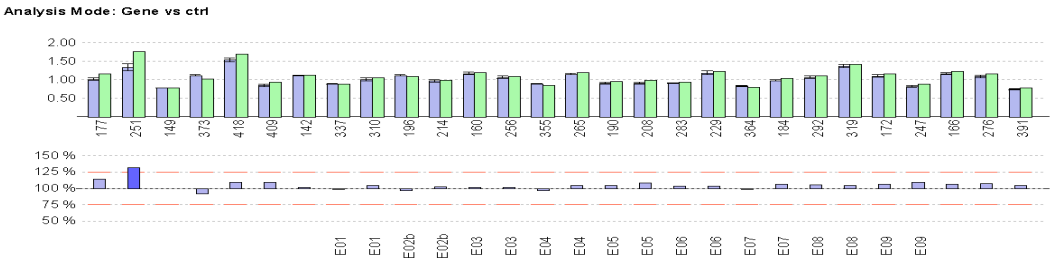

Figure 5 MLPA Results *SMARCB1* Kit: Patient 1 pBl

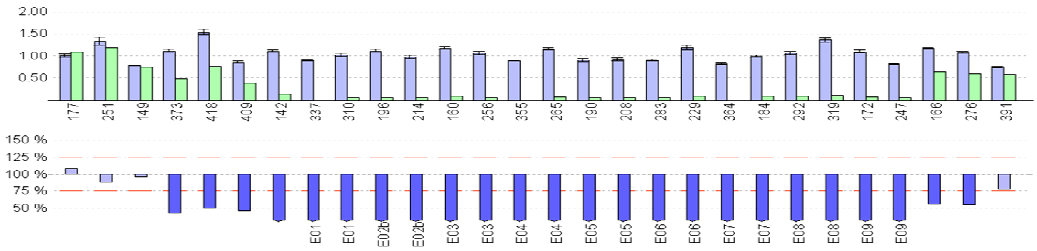

Figure 6 MLPA Results *SMARCB1* Kit: Patient 1 Tumor

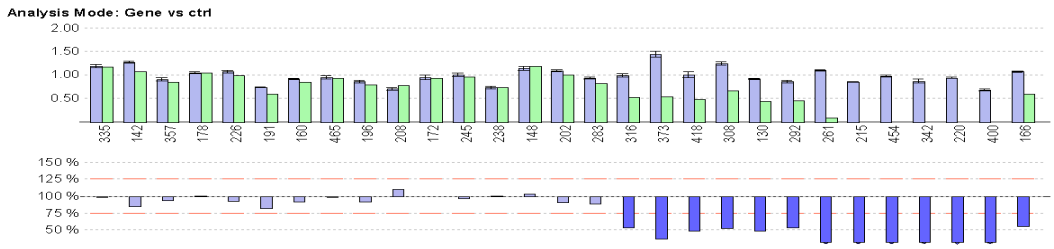

Figure 7 MLPA Results DiGeorge Kit: Patient 1 Tumor

MLPA results show that the homozygous deletion ranged from *GNAZ* to 93 nucleotides downstream of exon 9 of *SMARCB1*. The enormity of the heterozygous deletion could be further identified using SALSA MLPA kit 250 DiGeorge. By combining the results of both kits, the deletion ranges from *MED15* (DiGeorge) to *SEZ6L* (*SMARCB1*). Hypothetically there are two possibilites that the heterozygous and homozygous deletion could be distributed:

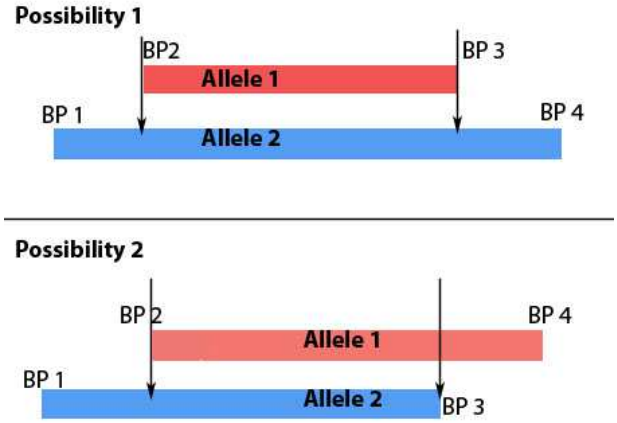

Figure 8 Hypothetical possibilities of deletion distribution among the two alleles, arrows point at the borders between homozygous and heterozygous deletion sites

Figure 8 Hypothetical possibilities of deletion distribution among the two alleles, arrows point at the borders between homozygous and heterozygous deletion sites displays the two hypothetical possibilities that the two deletions could be distributed among the two alleles of the patient. Possibility one depicts two deletions, different in size, one larger than the other. Possibility two describes two differently sized deletions that are suspended to one another. The arrows mark the homozygous deleted regions, which will appear accordingly

in the MLPA-results with 0% gene dosage. The flanking heterozygous deletions could be either on one allele alone or that both deletions are suspended to one another. The homozygous deleted regions were identified first, assuming possibility one were true. If that were the case, a deletion spanning PCR using a forward primer on the outskirts of breakpoint 2 (FWBP2) and a reverse primer on the outskirts of breakpoint 3 (RVBP3) would deliver the mutation sequence. However, several attempts using DreamTaq with and without DMSO, GoTaq with and without DMSO, Long Range dNTPack with and without DMSO, as well as inverted PCR and nested PCR did not deliver any sequencable band in the agarose gel. These results therefore, indicated that possibility two should be further investigated.

3.1.2 Breakpoint regions

Breakpoint one was subsequently narrowed down via real-time PCR. If possibility two proved to be true, a deletion spanning PCR using the forward primer of breakpoint 1 (FWBP1) and the reverse primer of breakpoint 3 (RVBP3) would reveal a sequencable band in the agarose gel electrophoresis. However, the tumor material proved itself contaminated with an unquantifiable amount of normal cells and wild type DNA from blood vessels nurturing the tumor mass. The unquantifiable amount appeared to distort heterozygosity. When 50% gene dosage was the case, an unquantifiable amount of wild type DNA in the tumor material would cause the actual gene dosage to appear falsely high, making it difficult to distinguish the difference between 100% and 50% gene dosage. The tumor material amplified variably, differing from run to run.

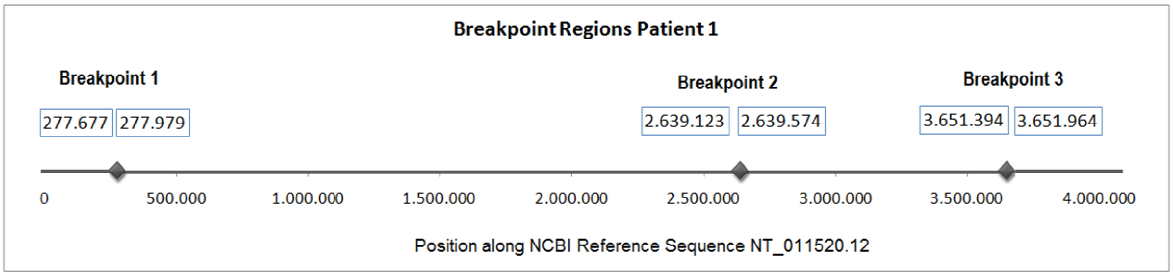

Figure 9 Patient 1 Breakpoint Regions 1 to 3

All of the primers named in the following are also listed in the Appendix under 8.6 List of Oligonucleotides and all positional information is given according to the NCBI Ref-

erence Sequence NT_011520.12. The supposed breakpoint 1 was narrowed down between primers 01_BP1_6.4 at position 277.677 and 01_BP1_6.4.5 at position 277.979. The supposed breakpoint region is 302 base pairs long. Whereas the breakpoint region of breakpoint two is 451 base pairs long, the supposed breakpoint 2 lies between primer 01_BP2_2.5.5 at position 2.639.123 and primer 01_BP2_2.5.4.3 at position 2.639.574. Breakpoint region 3 between primers 01_BP3_1.8.4 at position 3.651.394 and 01_BP3_1.8.5.2 at position 3.651.964 is 570 base pairs long.

3.2 Patient 2

Patient 2 presented himself at the age of thirteen months with an infratentorial tumor of the CNS. Histological analysis of the tumor material displayed a malignant neuroectodermal tumor composed of rhabdoid tumor cells with eosinophilic cytoplasm and eccentric nuclei with prominent nucleoli. The cell growth was described as unstructured without cribriform or papillary pattern. The mitotic activity was found to be brisk with small tumor necroses. Immunhistochemical analysis showed a loss of *SMARCB1*-expression within the tumor cells and a molecular genetic analysis via MLPA of the tumor material revealed a homozygous deletion within Exon 1 of *SMARCB1*.The patient had been lost before any kind of therapy could begin.

3.2.1 MLPA Results

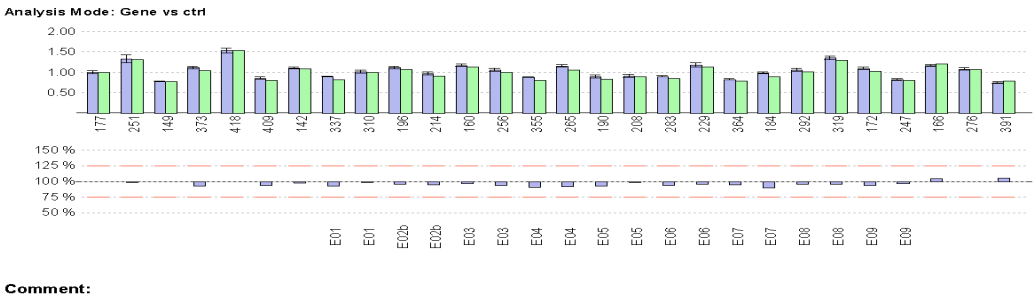

Figure 10 MLPA Results *SMARCB1* Kit Patient 2 pBL

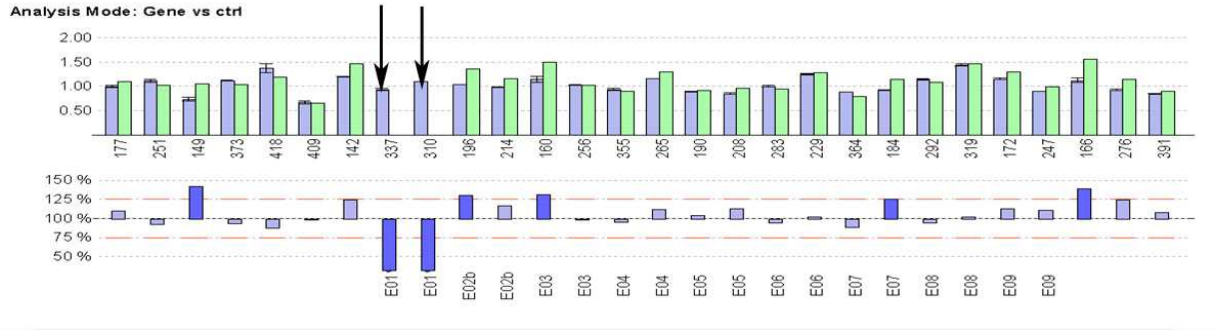

Figure 11 MLPA Results *SMARCB1* Kit Patient 2 Tumor, arrows point at the homozygous deletion within Exon 1

3.2.2 Breakpoint Identification

DNA from the patient's tumor was extracted from a FFPE-Block and peripheral blood DNA was extracted from a Guthrie-Card (Blood-Spot). A homozygous deletion within Exon 1 of *SMARCB1* was identified. The MLPA results narrowed the deletion down to 695.627 base pairs. Breakpoint 1 and breakpoint 2 were each narrowed down further with primer walking PCR using the GoTaqGreen Master Mix.

Subsequently, a deletion spanning PCR using the primers 02_BP1_12.12.6.3 forward primer (FWBP1) and 02_BP2_1.2 reverse primer (RVBP2) (see also List of Oligonucleotides in the Appendix) proved successful. The FFPE material amplified very inefficiently, however, which is why a reamplification of the PCR product was done.

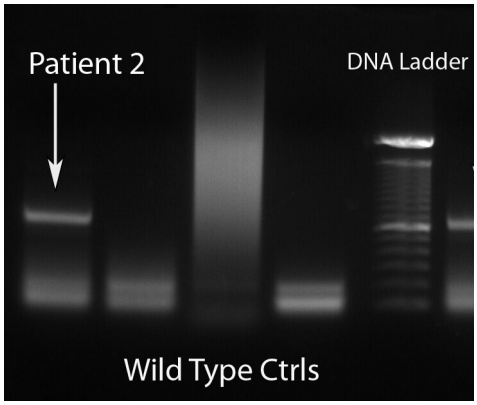

Figure 12 Patient 2 Agarose Gel Electrophoresis followingReamplification of deletion spanning PCR: Arrows point at a 600 bp band found only in Patient 2, not in the Wild Type Controls

Figure 12 shows the results of the reamplification. Two clear bands the size of 600 base pairs lift off from the controls. These bands were cut out and successfully sequenced.

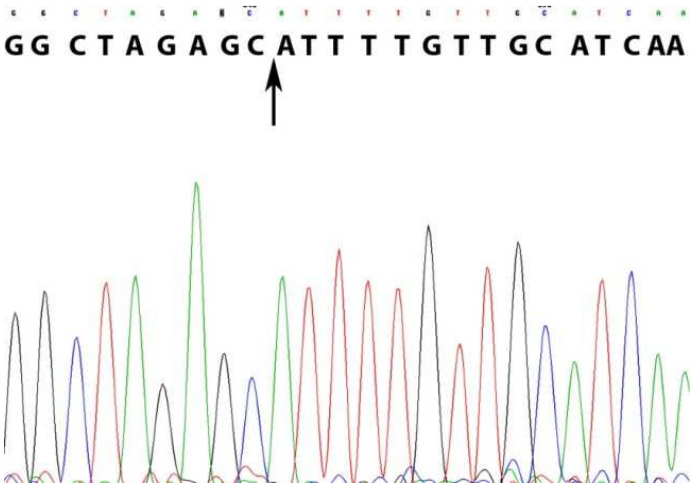

Figure 13 Patient 2 Breakpoint Sequence; arrow points at the fusion point where 5006 bp are deleted

Figure 13 shows an excerpt from the tumor DNA sequence, the arrow points at the fusion point of the deletion. 5006 base pairs are missing at the fusion point, which was discovered when comparing the sequence to the wild type NCBI Reference Sequence NT_011520.12 (NCBI).

3.2.3 Repeat Masking the Sequence

"RepeatMasker is a program that screens DNA sequences for interspersed repeats and low complexity DNA sequences." (Smit et al. 2010). The deleted sequence was masked for genomic interspersed repeats. The results did not reveal the existence of any long interspersed nucleotide elements (LINEs) flanking the sequence, however, the sequence contained 23,48% short interspersed nucleotide elements (SINES); 21,67% being Alu-sequences and 1,81 % so called mammalian-wide interspersed repeats (MIRs). Figure 14 depicts the fusion point of the deletion compared with the wild type sequence.

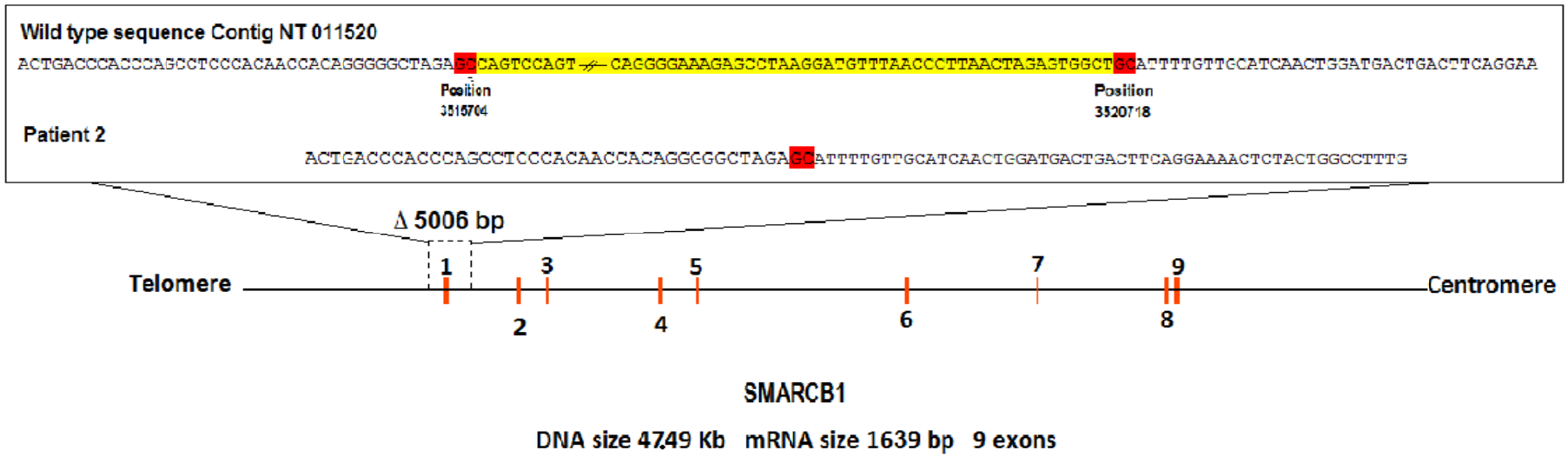

Figure 14 Patient 2 Fusion point

Below a map from Genatlas (Universite Paris Decartes ,1986). The wild type sequence Contig NT 011520 was compared to the tumor's sequence in the agarose gel band of patient 2. The red markings show possible mini-direct-repeat sequences, where non-homologous end-joining could have occurred following a DNA double-strand break. The yellow marked sequence represents the missing base pairs in the tumor (5006 base pairs in total).

3.2.4 Fragment Analysis

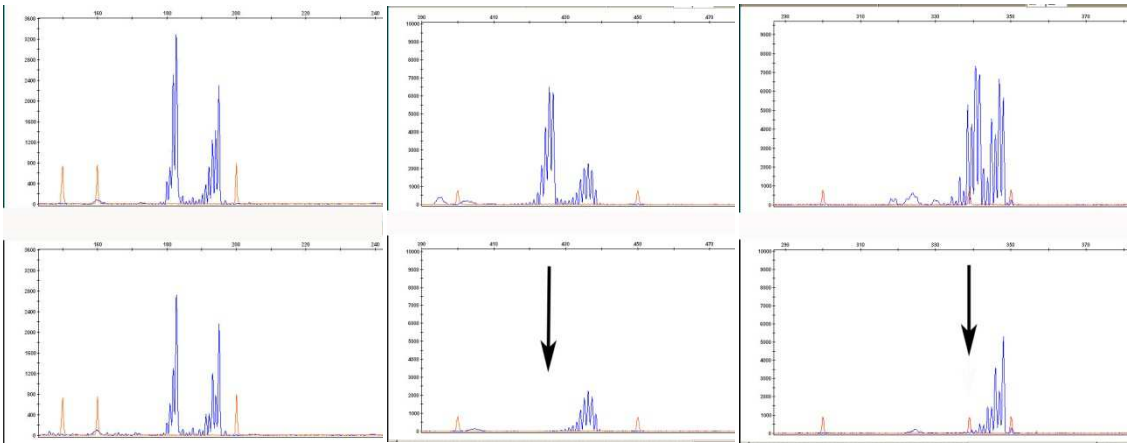

Figure 15 Primer pairs D22S425, D22S1174, D22S1169 for Fragment Analysis. Wild type (upper figures) vs. patient 2 (lower figures)

Fragment analysis results provided evidence for the hypothesis that a partial uniparental isodisomy is present in patient 2. Primer pair D22S425 is located upstream of *SMARCB1*, while primer pairs D22S1174 and D22S1169 are located downstream of *SMARCB1* (see also 8.3 Map of Oligonucleotides for Fragment Analysis in the appendix). While D22S425 shows two heterozygous alleles, like wild type, D22S1174 and D22S1169 primer pairs lack heterozygosity, displaying only one allele, indicating a partial uniparental isodisomy distal of *SMARCB1* exon 1.

3.2.5 Residual Tumor Cell Detection

A mutation specific forward primer was designed for the fusion point, a reverse primer 120 base pairs downstream from the forward primer. The primer pair was tested for specificity by performing a melting curve analysis with Quantifast SYBR Green Kit on the LightCycler Instrument. The primer pair proved specific for the mutation and therefore suitable for tumor cell detection using Quantifast SYBR Green on the LightCycler Instrument.

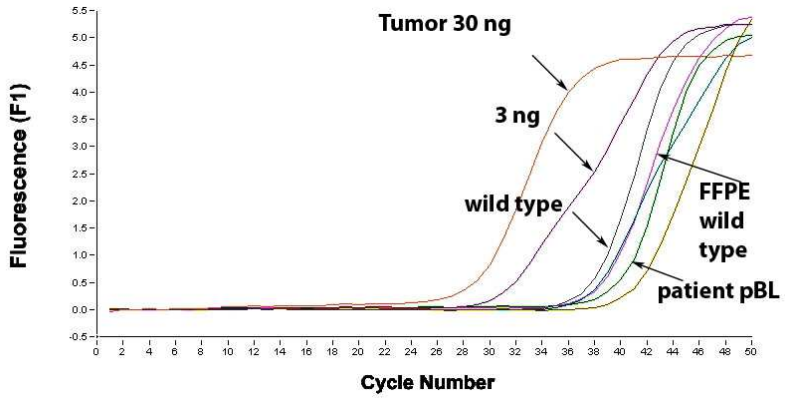

Figure 16 Residual Tumor Cell Search: Tumor vs. wild type and FFPE wild type controls vs. patient pBL

The results of the search for tumor cells in peripheral blood of the patient were negative. The negative results were previously anticipated, because AT/RT is a tumor of the CNS and therefore more likely to metastasize or release tumor DNA into the CSF, instead of peripheral blood of the patient. Unfortunately, the acquisition of CSF for research objectives for this patient was not possible due to the patient's early death.

3.2.5.1 Detection limit

A serial dilution of 1:10 of the tumor cell DNA in wild type DNA was prepared starting at a concentration of 30 ng/µl in the reaction vessel. Below a concentration of 3 ng/µl the wild type and FFPE-wild type DNA negative controls began to amplify and therefore signalized unspecific binding. Accordingly, it is appropriate to presume that the detection limit is at around a concentration of 3 ng/µl tumor DNA in a background of 30 ng/µl wild type DNA, which equals10 % tumor DNA in a background of wild type, respectively.

3.3 Patient 3

3.3.1 MLPA Results

The MLPA Results of patient 3 did not reveal any distinct deletions or gene dosage reductions along the sequence that was screened via MLPA Kit P258 *SMARCB1* and MLPA Kit P250 DiGeorge.

3.3.2 Mutation Identification

Two independent heterozygous mutations could be identified within *SMARCB1*, one on each allele, causing a biallelic alteration within *SMARCB1* in total. One allele carried a duplication of thirteen base pairs (see figure 17). The other allele carried a combined duplication of ten base pairs and an insertion of a single Guanine at the fusion point (see figure 17).

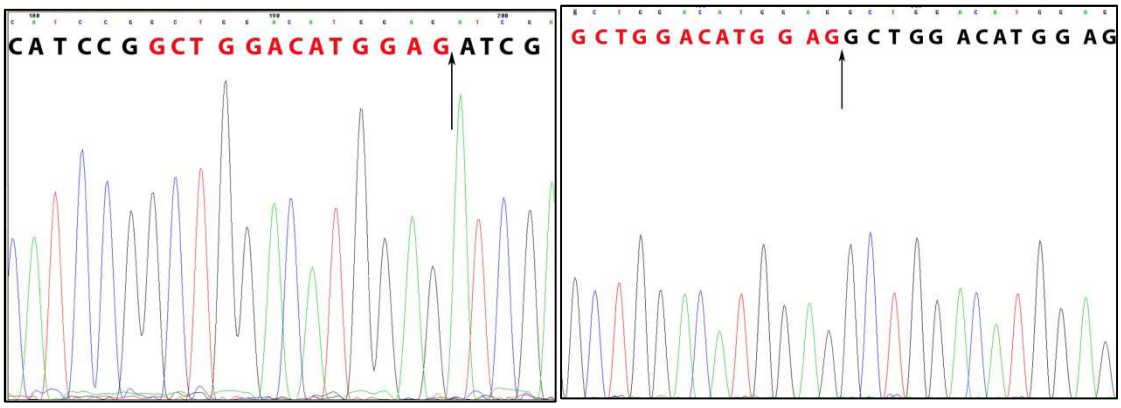

Figure 17 Patient 3 peripheral blood (left) vs. tumor (right). The tumor shows a duplication of 13 base pairs compared to the normal peripheral blood

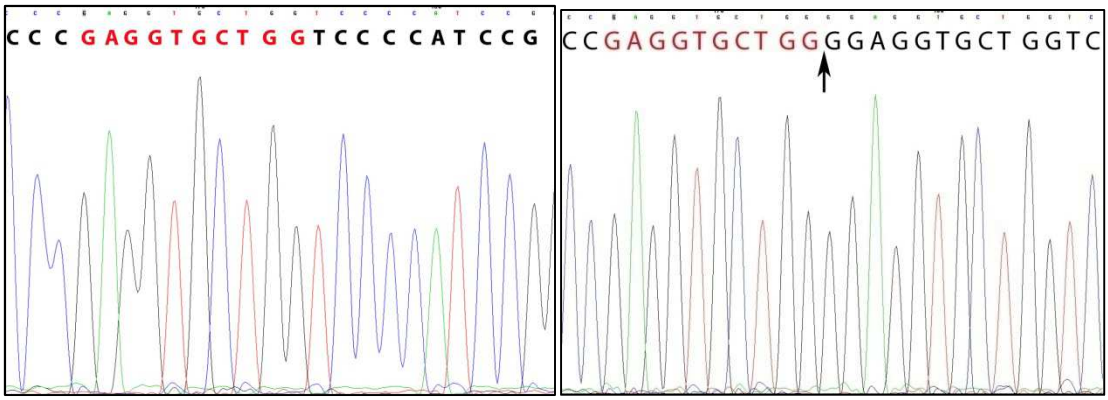

Figure 18 Patient 3 peripheral blood (left) vs. tumor (right). The tumor shows a duplication of 10 base pairs (red), the arrows shows the fusion point.

A total of three mutation specific primer pairs were designed for patient 3. Each of them was tested for specificity via melting curve analysis with Quantifast SYBR Green. The most specific primer pair was used for residual tumor cell search. The starting material for real-time PCR was FFPE-tumor tissue at a rather low starting concentration of only 1,38ng/µl.

3.3.3 Residual Tumor Cell Search

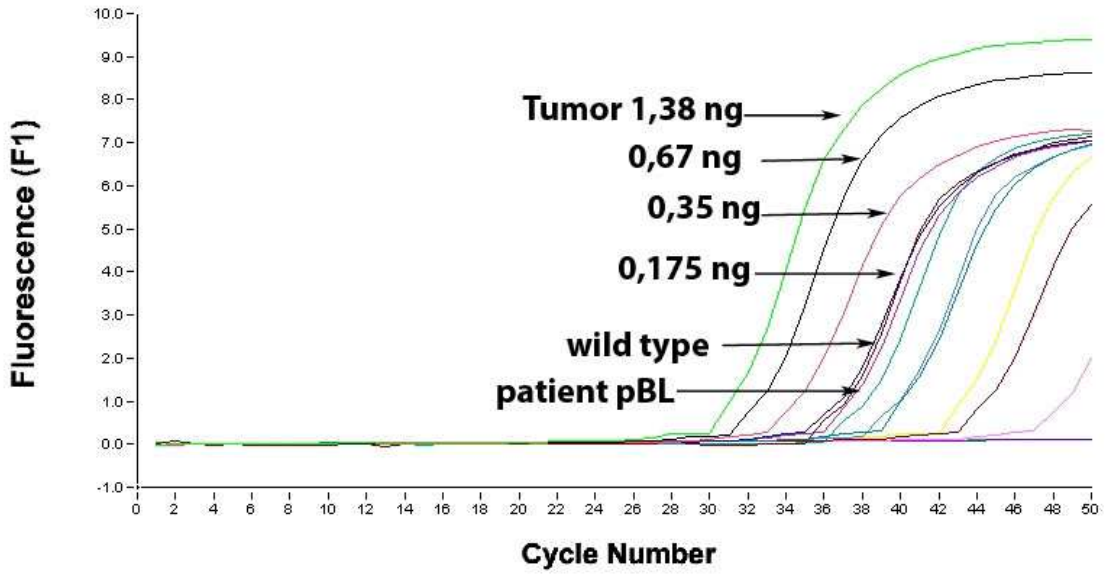

Figure 19 Residual Tumor Cell Search: Serial dilution of the tumor along with wild type and patient pBL (11 ng in reaction vessels)

A serial 1:1 dilution of the FFPE-tumor template DNA was performed starting at 1,38ng/µl. The residual tumor cell search via real-time PCR proved negative for tumor cells in the peripheral blood of the patient. Figure 19 shows that at a tumor cell quantity of 0,175 ng in the reaction vessel in a background of 1,38 ng/µl wild type DNA, unspecific primer binding occurs, as the negative wild type controls are equally amplified. The patient's peripheral blood DNA also amplified at the same concentration, which is why it can be concluded that either the patient's peripheral blood is negative of tumor cells or the amount of tumor cells in the peripheral blood lie below the detection limit. The detection limit is 0,35ng/µl. Serial dilution of the tumor starting with 1,38 ng (100%). 0,35ng/µl in a background of 1,38 ng/µl wild type DNA equals 18,11%.

3.4 Patient 4

Patient 4 was diagnosed with AT/RT WHO Grade IV at the age of 35 months. There is no further information available regarding clinical symptoms and the progression of the disease.

3.4.1 MLPA Results

A complete DNA sequencing of all *SMARCB1* exons was performed. The results revealed a homozygous deletion of two base pairs (Adenin and Cytosin) within Exon 6 of the *SMARCB1*-gene. The patient was diagnosed with rhabdoid tumor predisposition syndrome.

The patient's tumor tissue was also screened for deletions along the *SMARCB1* sequence using the SALSA MLPA kit P258 *SMARCB1*. The results of the MLPA showed a heterozygous deletion only in the tumor tissue ranging from *PPIL2*-probe to *NIPSNAP1*-probe. This deletion was not traceable in the peripheral blood of the patient. The heterozygous deletion and its breakpoints was not further examined, due to lack of patient sample material. However, this did not stand in the way of a residual tumor cell search because mutation specific primers could be designed for the homozygous deletion of two Adenin and Cytosin.

3.4.2 Mutation Identification

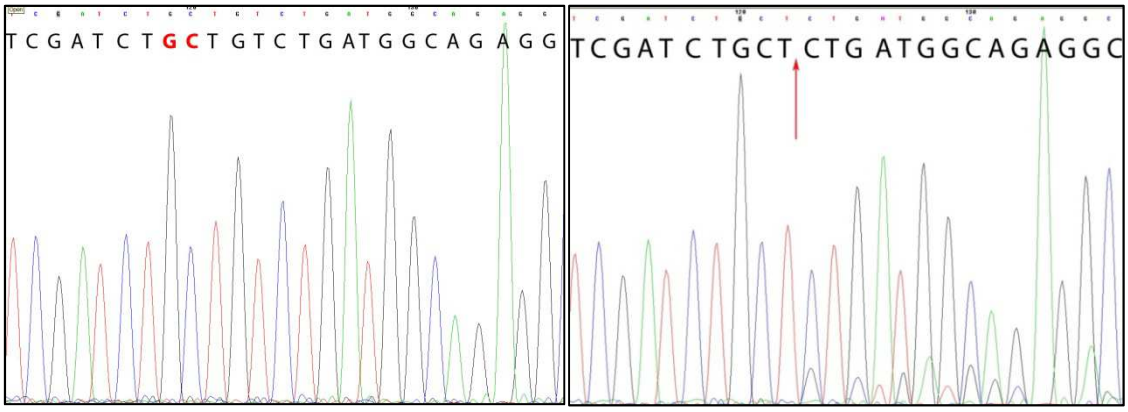

Figure 20 Patient 4 Mutation site. Peripheral blood (left) shows the wild type sequence, tumor (right) ARROW points at fusion point, a deletion of two base pairs (GT) in Exon 6

The mutation caused a frameshift and an early STOP-Codon within the Aminoacid-sequence. The arrow in figure 20, points at the fusion point; where two base pairs (GT) are missing. This fusion point was used for designing a mutation specific reverse primer and an upstream forward primer. The primer pair was tested for specificity via melting curve analysis.

3.4.3 Residual Tumor Cell Search

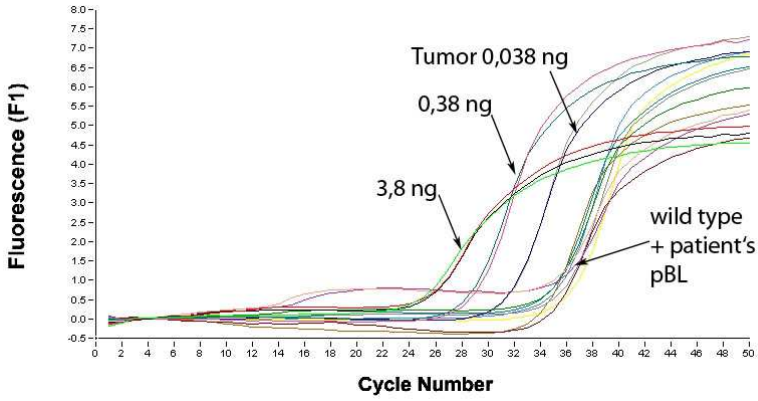

Figure 21 Patient 4 Residual Tumor Cell Search. Serial Dilution of Tumor (positive Ctrl.) along with wild type (negative control) and patient's peripheral blood (304 ng in reaction vessel)

The residual tumor cell search was negative of tumor cells in the peripheral blood of the patient. Here, too, a serial dilution of the tumor was done, to quantify any detectable amount of residual tumor cells. The negative controls were wild type, to distinguish

unspecific binding from tumor specific binding. The patient's peripheral blood contained 304 ng DNA in the reaction vessel. Despite the high amount of DNA provided, no tumor DNA could be detected, merely unspecific binding. The detection limit was determined with help of the serial dilution of tumor cell DNA. The starting concentration was 3,8ng/µl (100%) in the reaction vessel followed by a 1:10 dilution with wild type DNA at a concentration of 3,8 ng/µl. Below a quantity of 0,038 ng in the reaction vessel the wild type DNA began to amplify equally, the detection limit is therefore 0,038 ng in a background of 3,8 ng wild type DNA, which equals about 1 % tumor cells in a background of wild type DNA.

3.5 Patient 5

Patient 5 was first presented with a pontine mass with extensive hemorrhage and massive cell growth up into the left thalamus. Histological analysis displayed a malignant neuroectodermal tumor with high cell density and unstructured, compact cell growth and extensive necrosis. The small, but few, differentiated tumor cells did not display any rhabdoid differentiation. Subsequent immunohistochemical analysis showed negative expression of nuclear *SMARCB1* activity, while SMARCA4 activity was still intact. Furthermore the tumor cells showed cytoplasmatic and membrananous EMA-immunoreactivity but no expression of cytokeratin and GFAP. The patient was therefore diagnosed with AT/RT WHO Grade IV.

3.5.1 MLPA Results

The SALSA MLPA kit P258 *SMARCB1* results of patient 5 showed a homozygous deletion ranging from *GNAZ* to Exon 9 of *SMARCB1*. Also discernable in the MLPA results was that a not negligible quantity of wild type cells was amplifiable, indicating a relatively high contamination of the tumor material with wild type DNA. Furthermore, only 35 µl of 4,5ng/µl of tumor template DNA was available from the patient.

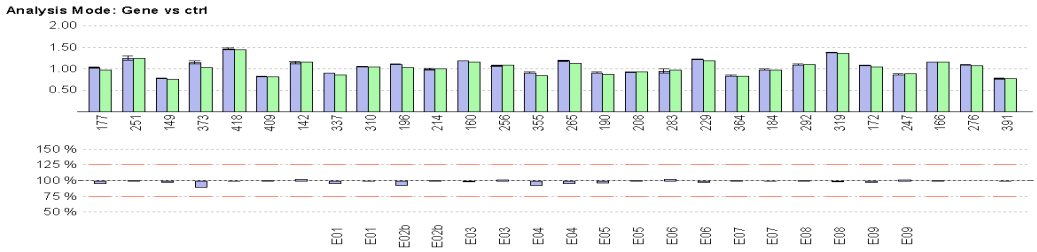

Figure 22 MLPA Results *SMARCB1* Kit Patient 5 pBL

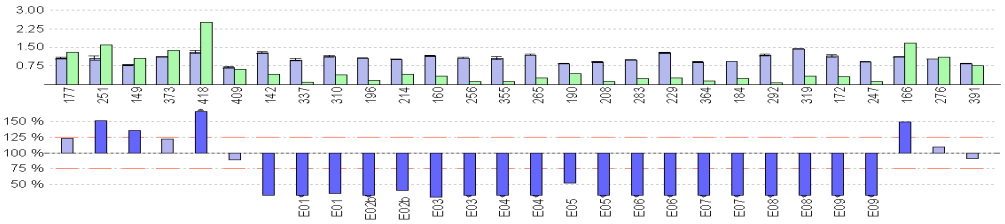

Figure 23 MLPA Results *SMARCB1* Kit Patient 5 Tumor

The DNA concentration was determined with a Qubit Fluorometer. The results let on that the material was probably too scarce and too low in quality, due to high contamination with wild type DNA, for a breakpoint identification, subsequent mutation specific primer design and residual tumor cell search.

3.5.2 Breakpoint Regions

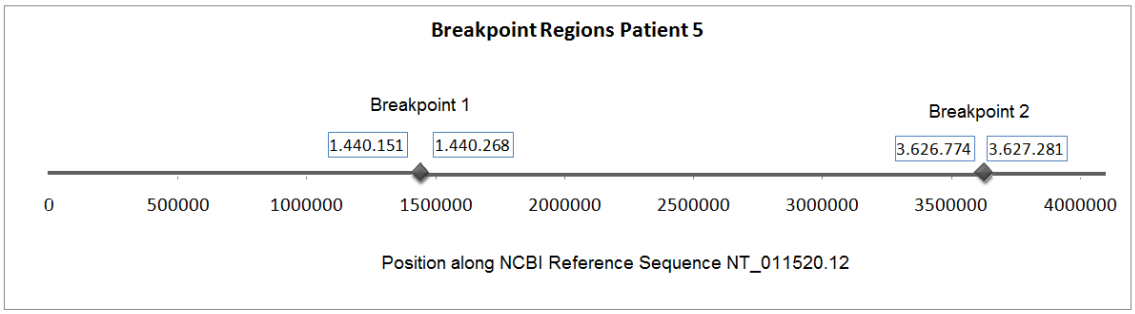

Figure 24 Patient 5 Breakpoint Regions 1 and 2

Homozygous deletions had proved to be best suitable for breakpoint identification in AT/RT-tissue, as was shown for patient 2. For this reason breakpoint identification was nevertheless attempted for patient 5, despite the unfavorable circumstance of lack of

quality and quantity of material. The breakpoint identification was, however, not possible. Following primer walking PCRs with GoTaqGreen Master Mix, several deletion spanning PCRs were performed, none of which delivered a band in the agarose gel electrophoresis suitable for sequencing. The breakpoint 1 is assumed to lie between primer 05_BP1_0 at position 1.440.151 and primer 05_BP1_1.0 at position 1.440.268. Primer walking results narrowed down breakpoint 2 between primer 05_BP2_8 at position 3.626.774 and primer 01_BP3_1.6 at position 3.627.281, a region of 507 base pairs.

3.6 Patient 6

Patient 6 was diagnosed with AT/RT at the age of four. No further information regarding clinical symptoms, location of the tumor and therapy is available for this patient.

3.6.1 MLPA Results

The SALSA MLPA kit P258 *SMARCB1* screening for deletions within the *SMARCB1* gene was negative. The results showed no alterations in peripheral blood or tumor tissue.

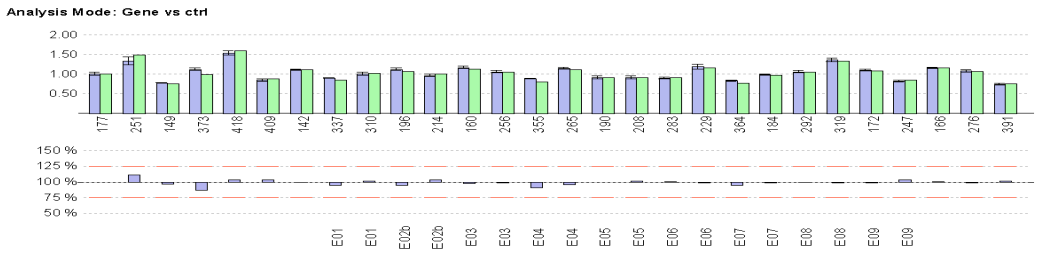

Figure 25 Patient 6 MLPA Results pBL

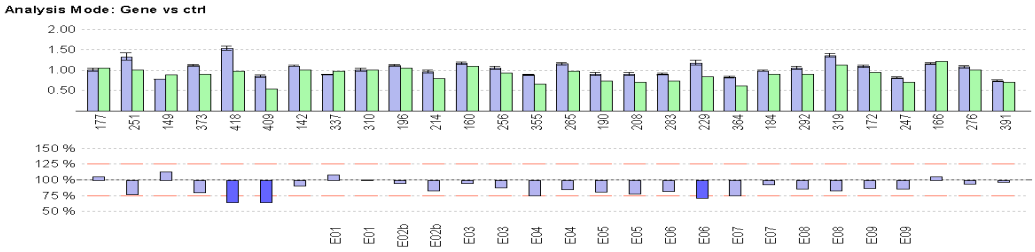

Figure 26 Patient 6 MLPA Results Tumor

3.6.2 Mutation Identification

A complete sequencing of all nine exons and flanking introns of *SMARCB1* was performed and the results showed a homozygous duplication of 43 base pairs in exon 5. The duplication had lead to a frame shift mutation and an early Stop-Codon in the amino acid sequence. The tumor material was highly contaminated with wild type DNA, which is why the tumor only amplifies very inefficiently. In figure 27 the red letters mark the tumor sequence that is only discernable as the smaller peaks in the sequence.

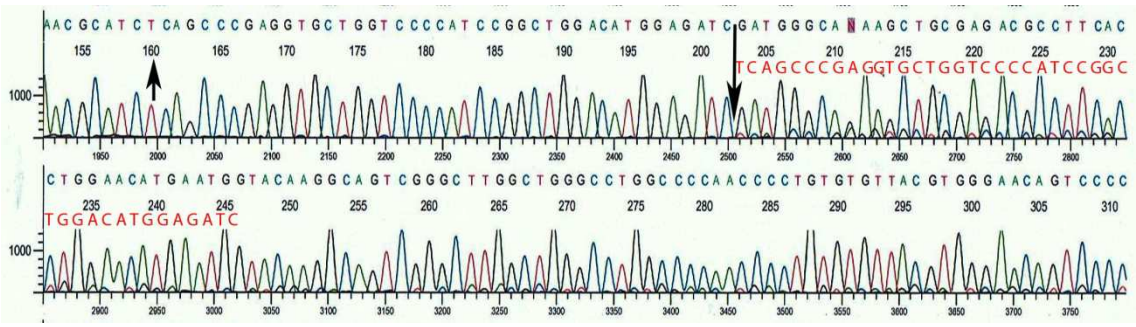

Figure 27 Patient 6, the small arrow points at the beginning of the wild type 43 base-pair sequence that is subsequently duplicated in the tumor big arrow)

A mutation specific forward primer was designed to bind at the fusion point of the duplication, while a reverse primer was designed downstream of the fusion point. In order to enhance the specificity of the primer product a 6-FAM-BHQ-1-marked probe was placed within the primer product.

3.6.3 Residual Tumor Cell Search

The tumor template DNA was predominated with wild type DNA, a circumstance that made specific residual tumor cell detection especially challenging. The mutation specific primer pair proved specific for the tumor template DNA in the melting curve analysis. A serial dilution from a starting concentration of 30 ng in the reaction vessel as shown in Figure 28 was performed. The results show that equal amplification took place for all dilutions of the tumor template DNA and wild type controls are also amplified in the same cycle of quantification.

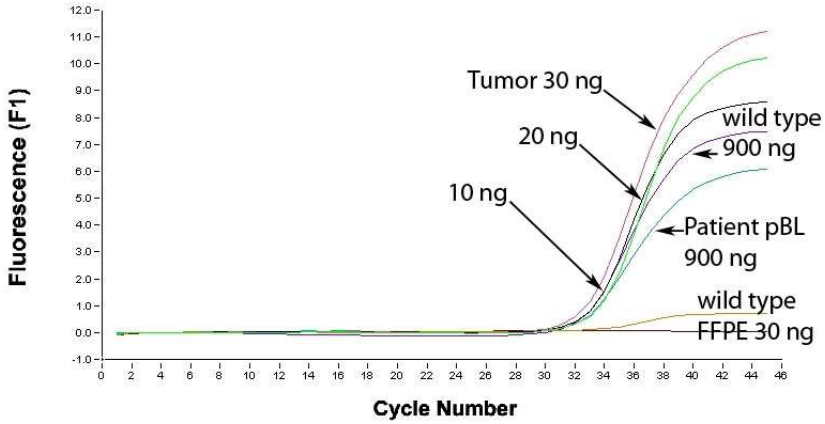

Figure 28 Residual Tumor Cell Search for Patient 6 Serial dilution of tumor DNA, wild type and patient pBL were inserted in very high concentrations

A serial dilution of the tumor DNA was done in order to determine the detection limit and to semi-quantify any detectable residual tumor DNA in the patient's peripheral blood. Wild type template DNA as well as DNA from the patient's peripheral blood was applied at very high concentrations (900 ng in the reaction vessel) in order to enhance the probability of detecting tumor cells. . However, the application of high amounts of DNA also enhances the probability of unspecific binding, which is clearly demonstrated in Figure 28. Both wild type and patient's peripheral blood DNA are amplified at the same rate, indicating that the 6-FAM-BHQ-1-dual-marked probe and the mutate on specific primers used are not specific enough to detect any residual tumor cells or that there are no tumor cells to be detected, respectively. The results indicate that the tumor tissue was too low in quality and quantity to enable specific amplification, which is why no significant differences between the different dilutions are discernable. There is no

statement to detection limit possible, because the purity of tumor DNA is not given and the remaining amount of tumor tissue is not quantifiable.

3.7 Patient 7

Patient 7, when introduced to the clinic at the age of 23 months, displayed newly occurred tilting of the head and neck, intermittent emesis, unsteady gait and a propensity to fall. Medical imaging revealed a tumor mass in the posterior fossa. Immunhistochemical staining revealed a loss of nuclear *SMARCB1*/INI1-expression in the tumor mass. For patient 7 the very ideal conditions were fresh frozen tumor tissue, peripheral blood and cerebrospinal fluid were provided.

3.7.1 MLPA Results and Mutation Identification

Subsequent molecular genetic analysis showed a large heterozygous deletion ranging from *TBX1* to *NIPSNAP1* in Exon 3 of *SMARCB1* on one allele, while the other allele contained a duplication of two base pairs. The duplication of Guanine and Thymin, was found at position 3.526.414/5, and caused a frame shift mutation and an early stop-codon. In sum, both mutations caused a biallelic alteration of *SMARCB1* on both alleles, fulfilling Knudson's two-hit theory for tumor suppressor genes.

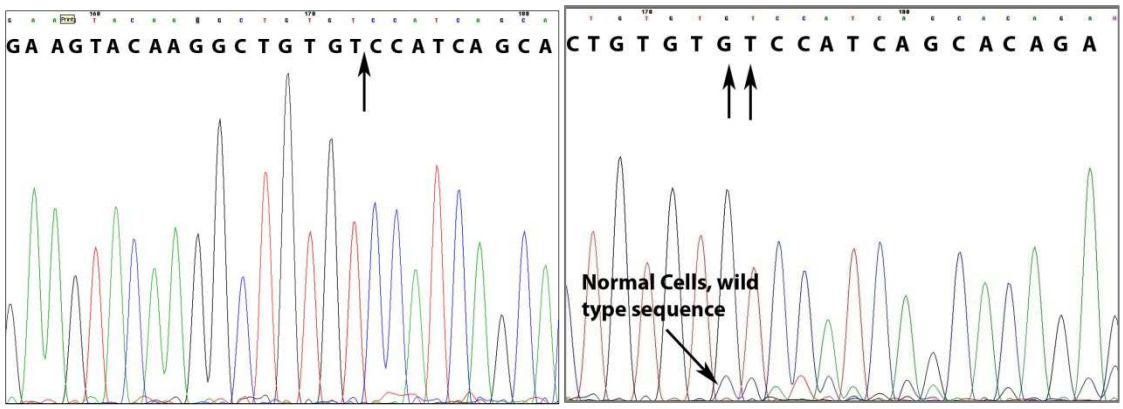

Figure 29 Patient 7 Peripheral Blood(left) vs. Tumor (right), arrows point at the duplication site, two base pairs (GT) have been inserted, the tumor sequence is shifted against normal cell sequence

3.7.2 Residual Tumor Cell Search

Two mutation specific primer pairs for the two base pair duplication were designed. Both were tested for specificity via Quantifast SYBR Green PCR melting curve analysis.

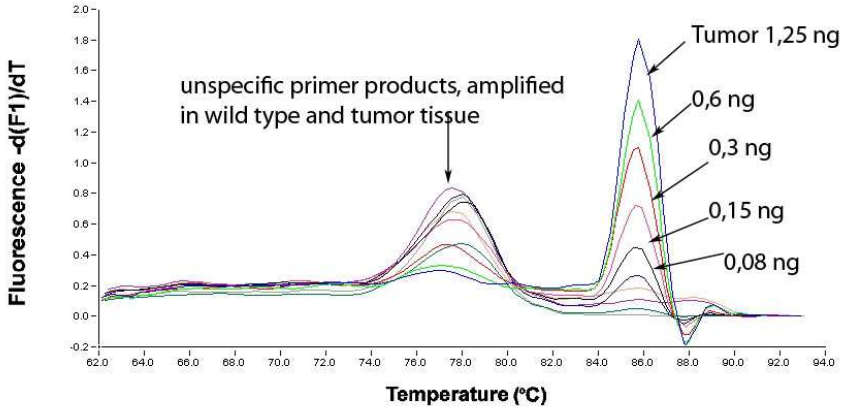

Figure 30 Patient 7 Melting Curve Analysis of Light Cycler PCR-run testing the primer specificity tumor vs. wild type. The unspecific primer products can be canceled out using a dual-marked probe.

Figure 30 shows the results of the melting curve analysis. The melting curve analysis shows two different primer products that differ in size, recognizable by the two distinct peaks. The first, smaller peak is due to unspecific amplifications, while the more significant peak on the right represents the actual tumor cell specific product. It can be assumed that both PCR-products contribute to fluorescence detection during amplification. In order to cancel out fluorescence detection deriving from the unspecific products a 6-FAM-BHQ1-dual-marked probe was placed within the tumor template DNA sequence. A dual-marked probe will only emit a fluorescence signal, if the tumor cell specific product is being amplified. Whereas the unspecific product will nevertheless be amplified, however, remain undetected.

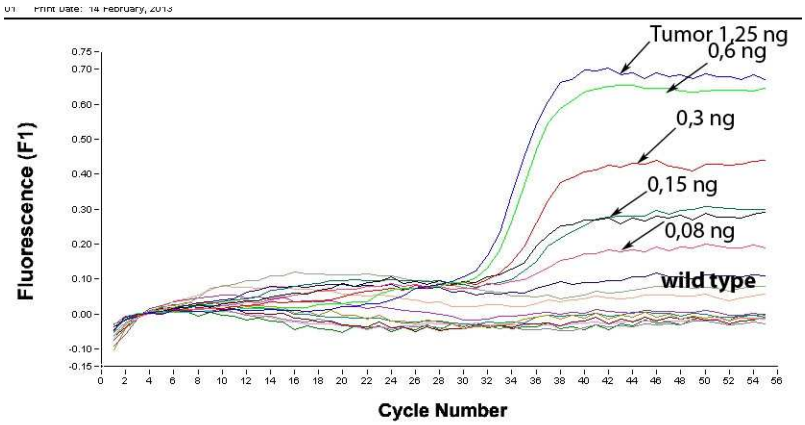

Figure 31 Patient 7, Light Cycler PCR using 6FAM-BHQ1-dual-marked probe, Serial Dilution of tumor and wild type DNA.

Once the primer pairs were optimized at an annealing temperature of 61°C, a serial dilution of the tumor template DNA was performed. Figure 31 depicts the dilution series and how specific the primer products were. Wild type controls did not amplify at all.

The residual tumor cell detection consisted of the dilution series of the tumor DNA and an increasing amount of patient peripheral blood DNA (269 ng/µL, 538 ng/µl, 807 ng/µl) and CSF (0,5 ng/µl, 1 ng/µl, 1,5 ng/µl, 2 ng/µl). 10 µl reaction mixes were used. Despite having applied increasing amounts of peripheral blood DNA or CSF DNA, all results proved negative of tumor cells. The great advantage was that fresh frozen tumor was used for PCR and therefore peripheral blood and liquor as well as wild type DNA were directly comparable to one another, as there was no difference in DNA quality evident.

The detection limit was 0,08 ng tumor template DNA in the background of 1,17 ng wild type DNA in the reaction vessel of 10 µl. A serial 1:1 dilution was performed starting with 1,25 ng Tumor DNA (100 %). 1:1 dilution with wild type DNA at a concentration of 1,25 ng/µl. 0,08 ng of 1,25 ng is 6,4 % tumor cell detection limit in a background of wild type DNA.

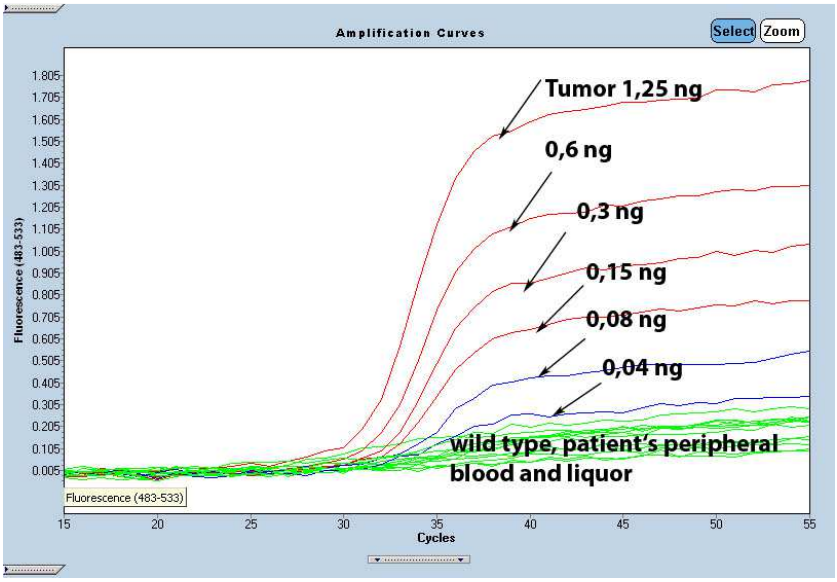

Figure 32 Residual Tumor Cell Detection with Light Cycler System 480 Instrument II, a dual-marked probe for higher specificity was used: wild type, patient's peripheral blood and liquor are negative of tumor cells. Nachweisgrenze: 0,08 ng in 10 µl reaction vessel (red = positive, blue = marginal, green = negative)

Results of the residual tumor cell detection with a dual-marked probe show that wild type controls, the patient's peripheral blood as well as CSF are negative of tumor cells. The tumor cells could be detectable down to 0,08 ng in 10 µl reaction vessel. Assuming a mass of 6,57 pg genomic DNA per single diploid cell (Serth et al. 2000), 0,08 ng/10 µl would be equivalent to 1,22 cells/µl detection limit.

4 Discussion

Molecular profiling is increasingly becoming a central research area in the field of oncology. Currently there is scientific consensus that cancer is generated by a multitude of genetic alterations in a series of oncogenes or tumor suppressor genes. A characterization of these alterations for each individual tumor, so it is assumed, will allow the prediction of clinical and biological behavior of any tumor type based on its molecular characteristics and thereby allow targeted individualized treatment in the future (Ichimura et al. 2012). The atypical teratoid rhabdoid tumor has obtained a special position among the different tumor entities because of its distinct pathogenesis and its association with a tumor suppressor gene: *SMARCB1*. Hasselblatt et al. (2013) and Kieran et al. (2012) screened AT/RTs for genetic alterations other than *SMARCB1* and found none. The evolution of cancer cells frequently leads to the formation of multiple clones due to most cancer types' high genetic instability. These clones are often able to escape detection or targeted treatment, under these premises any molecular marker would eventually become functionless. However, Lee et al. (2012) have found the biallelic loss of *SMARCB1* as genetically stable, which not only affirms the high specificity of the gene but also makes it an ideal molecular marker.

4.1 Deletion Mapping

The breakpoint regions of patient 1 and 5 as well as the identified breakpoints of patient 2 have been compiled in a single map (Figure 33) to reveal possible breakpoint accumulations. It is probable that this region may be more liable to DNA double strand breaks than others. These DNA double strand breaks are often followed by repair mechanism pathways that can result in allelic loss of nucleotides causing deletions. The total number of patients in this research objective is too small to propose a significant breakpoint accumulation at positions 3.519.779 – 3.651.964; however the results seem striking and indicate such. Further examinations of this chromosome band with more patient samples could confirm the region as especially liable in the future.

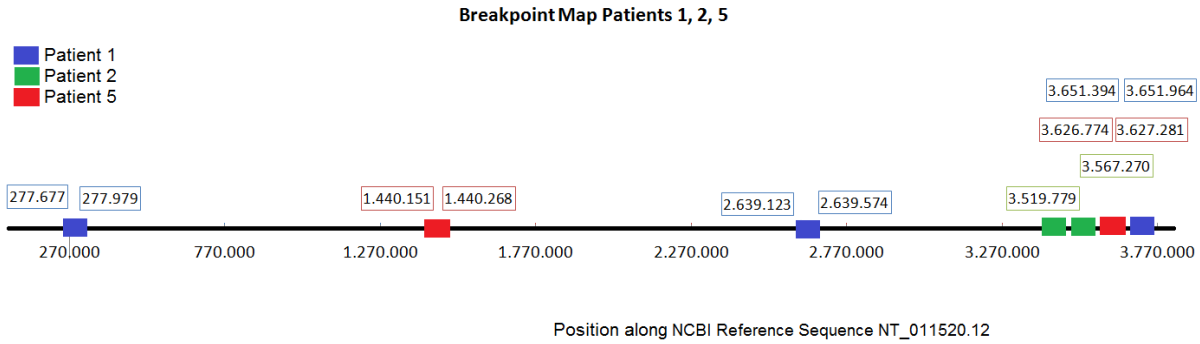

Figure 33 Breakpoint Map of Patients 1, 2 & 5

4.2 Patient 2 Repeat Masking and Fragment Analysis

The masking results of the deleted sequence in the tumor of patient 2 suggested a non-homologous-end-joining mechanism with the loss of nucleotides (see also 1.5.1 for DNA Repair Mechanisms). The Guanine and Cytosine, which are marked red in figure Figure 13 Patient 2 Breakpoint Sequence; arrow points at the fusion point where 5006 bp are deleted, could have functioned as sequences of micro homology, so-called mini-direct repeats (MDRs), where after a DNA double strand break may have occurred, NHEJ-pathway repair using the MDRs, resulted in the loss of 5006 nucleotides. This was probably the mutation mechanism of the deletions.

The deletions are likewise existent on both alleles, a rather singular observation, because two identical mutation mechanisms must have taken place on both alleles. This is regarded as a rather improbable event; more likely a double stranded DNA break occurred on one allele, was repaired via the NHEJ-pathway and another event, independent of the first, ensued. The second event may have resulted in a uniparental isodisomy, i.e. both homologous chromosomes derive from the same parent. This mechanism was further investigated by fragment analysis of the region on chromosome 22. The results revealed a partial uniparental isodisomy that begins at exon 1 of *SMARCB1* and continues downstream of the gene.

4.3 Residual AT/RT Cell Detection

Minimal residual disease (MRD) in solid tumors is challenging but also one of the main topics in clinical oncology (Pantel 1996) MRD was first established for acute lymphatic leukemia (ALL), a hematologic malignancy. The ALL patient's peripheral blood naturally swamped with mutant cells. In contrast, solid tumors, such as AT/RT, must yet release the tumor cells or mutant DNA, into the blood stream. The release mechanisms are not yet clearly understood. It is known that fragments of DNA circulate in the blood stream. Reasons for their presence could be apoptosis or necrosis of tumor cells and subsequent release of DNA fragments into the blood stream or the release of intact cells into the blood stream where they are subsequently lyzed (Gormally et al. 2007). Furthermore, the release of intact tumor cells could lead to metastasis; however, not all tumor cells in the blood stream are metastatic. The complex model of metastatic cells was described in chapter 1.4.1 Molecular Markers for Cancer. These challenges play a decisive role in developing methods that predict the presence of cancer for solid tumors such as AT/RT.

A further objective in clinical pathology is to develop suitable molecular markers for residual tumor cell detection. There have been a series of methods put forward, such as immuncytochemical assays using monoclonal antibodies (Pantel 1996) as well as the detection of mutations in oncogenes or tumor suppressor genes that are specific to a certain tumor type via polymerase chain reactions. The trouble is finding a suitable marker that is sensitive as well as specific for a tumor type. These criteria are being met in full when applying this method for residual tumor cell detection for AT/RT.Tumor specific mutation identification prior to residual tumor cell search in peripheral blood and CSF make it highly specific and the detection via real-time-PCR can be extremely sensitive, studies have revealed detection limits of 1 cell in 10^6 to 10^8hematopoetic background cells (Zippelius et al. 2000).

The results of residual AT/RT detection provide evidence that it is principally possible to use mutation specific primers to detect AT/RT cells in peripheral blood or CSF of the patient. The method is specific for each individual patient's tumor cells and can be optimized to enhance sensitivity. A definitive proposition concerning the detection limit,

i.e. sensitivity of the method, however, is not possible at the time. The sensitivity of the method must be probed under standardized circumstances for patient sample taking, uniform DNA extraction methods and the condition that clean fresh frozen tumor cell material without wild type DNA contamination be provided. Furthermore, the interpretation of quantitative results is yet unclear. The quantitative results differ considerably among the five patients tested for this research objective, due to the enormous differences in quality and quantity of starting material and other reasons that will be discussed further in 4.4 Limitations and Methodical Constrictions.

The detection limit was calculated via the concentration of tumor cell template DNA in a background of wild type DNA. In the group of five patients the calculated detection limit ranged from 1% - 18,11%. (Gormally et al. 2007) reported of similar numbers, “when mutant and wild-type DNA are mixed together prior to PCR, an experimental condition, which reproduces the analysis of actual biological specimens”, sensitivities of 1-6 % are reached (Gormally et al. 2007). However, the calculations are only valid under the presumption that the tumor material consisted purely of tumor DNA. Very probably this was not the case, as extracted DNA from solid tumors is often contaminated with normal cell DNA and wild type DNA from blood vessels nurturing the tumor mass, it can be assumed that the amount of tumor cells in the reaction vessels was lower than indicated and that the sensitivity of the method was actually higher than calculated for each patient. Furthermore, it must be noted that quantitative results should be linked to a cell number or more importantly, relevance for therapy or prognosis in the future.

4.3.1 Patient Follow-Up Results

A patient follow-up inquiry at the EU-Rhab Register was performed in March 2014 after all the experiments had taken place. Table 12 gives an overview of the patients’ metastatic status at the time of sample-taking in contrast to follow-up data concerning their disease progression. At the time of patient sample-taking the metastatic status of all seven patients was negative, except for patient 2. Patients 1 and 7 were relapse free, patients 2 and 3 deceased. Patient 4 suffered from intracranial metastasis and patient 5 had a massive tumor progression. No patient follow-up data was available for patient 6. The negative results of tumor cell search for six of the patients are consistent with this

information. As formerly discussed, metastasis would most likely be found in cerebrospinal fluid than in the peripheral blood of the patients. No cerebrospinal fluid had been available for tumor cell search from patient 2, which may explain the inconsistent results. The use of CSF for tumor cell search may offer more insights in the future.

Table 12: Patient Follow-Up Results received from EU-Rhab Register

Patient No°	Metastatic status at the time of sample-taking	Validation method	Follow-up: Disease progression
1	M0	MRT/CSF Cytology	no relapse
2	M2b/M+	MRT/CSF Cytology	deceasd
3	M0	MRT	deceasd
4	M0	MRT/CSF Cytology	intracranial metastasis
5	M0	MRT/CSF Cytology	massive tumorprogression
6	n/a	n/a	n/a
7	M0	MRT/CSF Cytology	no relapse

4.3.2 Ambiguity of Positive Results in Residual AT/RT Cell Detection

Positive results in residual AT/RT cell detection are ambiguous. Further research on the release mechanisms of tumor cells or DNA into the blood stream will facilitate the interpretation of MRD results in solid tumors in the future. Presently, the detection of tumor DNA in the blood stream must not be indicative of the presence of metastatic cells, as the cells may have acquired the ability to enter the blood stream but they must not have acquired the ability to extravasate (Gormally et al. 2007).

Gormally et al. (2007) also noted that the detection of mutant DNA is not informative of the tumor site, however, this information is rather secondary in this research objective, as the mutation specific primers are specific for the primary tumor site and AT/RT are known to be genetically stable (Ichimura et al. 2012).

The detection of circulating tumor cells in peripheral blood or cerebrospinal fluid, once successfully established and standardized, will be an alternative to invasive biopsies or surgical exploration. The spectrum of application will range from the early diagnosis of primary tumors, the detection of metastatic tumor tissues, the monitoring of cancer pa-

tients and also prognostic factors concerning survival and predictive response to cancer therapy especially development of therapy resistance could be monitored (Parkinson et al. 2012).

Until then a series of questions will have to be answered prior to its introduction to clinical pathology. What propositions concerning sensitivity of the method can be made? What consequences will a positive result have and where would the therapeutic threshold begin? It must be noted at this point, that any positive result in any screening method is obsolete, if no effective therapy can follow. This circumstance demands the development of better therapeutic and prognostic factors for AT/RT patients. How does tumor progression relate to the positive results and how should the latter be quantified? Finally, the method must be more sensitive and specific than contemporary conventional methods, such as medical imaging, in order to be profitable for the patient as well as the physician.

In order to introduce this detection method into clinical practice, a number of standardized protocols need to be developed and agreed to as well as multi-center studies will be required for validity (Pantel 1996).

4.4 Limitations and Methodical Constrictions

4.4.1 Scarce material

One of the greatest limitations during the entire experiments was the scarceness of tumor-DNA and its poor quality. AT/RT is a rare tumor entity. Once the seven suitable patients were found, a sufficient amount of material was required for the experiments. However, as AT/RT is rare and the patients' prognosis very grim, an extensive amount of material was not obtainable, as some patients had deceased before experiments had begun. Furthermore, the quality (fresh frozen, FFPE, different DNA extraction methods, etc.) and quantity varied tremendously among the patients, making a direct comparison difficult or impossible. Future research objectives should attempt to minimize these differences and ensure a uniform quality and quantity of sample templates. The attempt to amplify the tumor material with a whole genome replication kit (see 0 List of Instruments and Materials of the Appendix for further details) did not yield any suitable material for this research objective.

Ideally, a whole series of mutation specific primer pairs should be designed and tested for each individual tumor type, because primer pairs tend to differ in binding behavior and annealing temperatures and therefore influence PCR efficiency. The best primer pair with the highest specificity should be applied for residual tumor cell detection. This procedure ensures the best possible residual tumor cell detection. However, the scarceness of material often allowed only a few real-time-PCR runs testing one or two primer pairs, at 60°C annealing temperature. The real-time-PCR runs were nevertheless successful; they clearly demonstrated that *SMARCB1* mutations are suitable molecular markers for residual tumor cell detection in AT/RT. These results are sufficient for a proof-of-principle.

4.4.2 Working with FFPE-Material

Formalin-fixating-paraffin-embedding is one of the most convenient, long-lasting and therefore most commonly used methods for preserving tissue. However, formalin-fixation and paraffin-embedding significantly reduce the quality of the DNA. For many

research objectives this circumstance is no actual impediment but for molecular genetic analysis it is. Highly fragmented material is difficult to analyze if the sequence in question is large, such as large breakpoint regions.

When narrowing down the breakpoint via primer walking, wild type DNA extracted from lymphocytes from a human vein was used as a positive control for PCR-cycling. Due to the fact that DNA extracted from FFPE-material amplifies less efficiently than wild type DNA, the tumor band in the agarose gel electrophoresis would naturally be darker than that of the wild type, even if starting templates were adjusted equally. In addition, a contamination of tumor tissue with wild type DNA could create false-positive results, feigning gene existence in the tumor, when actually the primer pair lay within the deleted region. Ergo, primer walking results were only informative when flanking primer products were compared to one another and the deletion spanning PCR delivered a plausible sequence.

Furthermore, the reduced quality of DNA had severe impact on real-time-PCR efficiency and comparability. FFPE-DNA will amplify up to one log-phase or three cycles later than fresh frozen tissue of the same template amount.

4.5 Real-Time PCR Quantification and Real-Time PCR Kinetics

Real-time-PCR technology has the capacity to detect and quantify minute amounts of nucleic acids. However, its high sensitivity makes it susceptible to errors in analysis as well as in the interpretation of results. Small differences in assay runs can have a significant impact on its validity and the interpretation of quantitative experiments can be challenging due to minute variations in template amounts in the reaction vessels due to pipetting errors. The efficiency of a real-time-PCR run can be limited by experimental factors such as initial concentrations of starting material of all substances in the reaction vessel, the degradation of TaqPolymerase, PCR product reannealing and primer-dimer accumulation (Roth et al. 2002). Furthermore, real-time-PCR efficiency is highly sensitive to differences in DNA quality and quantity, which is why it was an utmost necessi-

ty to uniformly determine DNA-concentration via Qubit Fluorometer before setting up the PCR-reactions.

4.5.1 Relative gene quantification real-time PCR for Primer Walking

Relative gene quantification for patient 1 used Livak and Schmittgen's (2001) $2^{-\Delta\Delta Ct}$ - Method, where Ct stands for the threshold cycle or cycle of quantification and the factor two refers to a perfect efficiency at each quantification cycle (Gevertz et al. 2005). The factor two therefore, implies that both genes, the reference gene as well as gene in question, are both amplified with the same efficiency. Small deviations from the factor two can be corrected using an error calculation formula:

$$\textit{efficiency deviation} = \frac{2^n}{E^n} - 1x\ 100$$

(Schakowski 2012).

The amplification efficiencies probably did not match the factor two during the experiments, because an undetermined amount of wild type DNA contaminated the tumor material causing a deviation from the factor two. Further influential factors are primer design, annealing temperatures, fragment length, amplification sequence, GC-amount, purity of DNA, inhibitors, NA degradation, PCR program, PCR reaction components (Schakowski 2012). Besides, the factor two is only a mathematical approximation and does not mirror actual PCR reality, which is why Gevertz et al. (2005) developed a mathematical model of real-time PCR kinetics that could calculate PCR efficiency as a function of cycle number. This is required, when quantifying minute differences between samples. Evidently, there is yet much room for optimization in using relative gene quantification real-time PCR for breakpoint identification. However, the amount of patient samples did not suffice for this. Future research objectives, however, should consider both the mathematical models as well as the limiting factors named above more intensively.

4.5.2 Real-time PCR Fluorescence Detection

The real-time PCR analysis program detects fluorescence signals (y-axis) and plots the signal against cycle number (x-Axis). The curves that result in the process can be erratic

or irregular (see figure 29). A consultation with the manufacturer Roche Applied Science, Mannheim (specifically Dr. Canino), revealed that these phenomena often occur due to external disturbances, such as shaking tables and nearby running centrifuges, during the real-time PCR run. The Cq points required for quantification remain undisturbed through these irregularities.

4.6 Patients 1 and 5

Tumor samples of patient 1 and 5 were designated for breakpoint identification. However, despite having narrowed down the breakpoints, no deletion spanning PCR proved successful. Possible reasons were that the deletions were very large, as shown in the MLPA results but also a low quality of the material.

When examining the tumor material of patient 1, an obstacle may have been the heterozygous deletion where the gene dosage quantification via real-time PCR was unsuccessful. Furthermore, there is reason to believe that more complex mutation developments have taken place in the tumor. The assumed distribution of deletions and mutations among the two alleles of patient 1 seem to have been false. Perhaps insertions, inversions or non-consecutive deletions are responsible for the ineffective deletion spanning PCR. These supposed impediments cannot be proven under the circumstances given, which is why they will remain thoroughly hypothetical. Tumor samples of patient 5 showed homozygous deletions on both alleles, however, the amount of patient samples was surely too scarce, the tumor tissue was additionally highly contaminated with wild type tissue, therefore the quality proved too low for an effective amplification. Nevertheless, these two cases well display the limits of this research objective and further suggest possible hindrances that need to be considered in future projects.

4.7 Future prospects: Identifying Molecular Markers to predict the Presence of Cancer

With increasing computing capacity, more efficient processors and greater data-storage devices, it will only be a matter of time that we develop the according algorithms to

specifically analyze the human genome and perhaps one day we will be able to predict events, the patients' response to therapy and on the grounds of these findings, perhaps even prevent complications. We are on the verge of individualized medicine, in order to pave the path toward these new chances, molecular profiling will gain more and more impact and weight. Understanding the dynamic behavior of tumor oncogenes and suppressor genes will be inevitably a future central discipline. And with higher curability and these new possibilities the expectations on and demands for a physician will inevitably grow, as Sherry Phillips stated "With steady increase in survival rates for children with cancer, those who provide their medical treatment face new challenges. In the past, it was acceptable to treat the malignancy and to be satisfied that the child survived. Now, the goal of treatment is to achieve a totally cured child, defined as one who is mentally as well as physically healthy and can function in society. Thus our responsibilities extend beyond simply rendering our patients free of disease […] We must ensure that patients are able to grow and develop and realize their greatest potential."(Phillips 1989).

5 Summary

Atypical teratoid rhabdoid tumors are a highly malignant and aggressive pediatric embryonal tumor entity of the central nervous system. The tumor entity has been distinctly linked to genetic alterations on both alleles of *SMARCB1*. The current state of research provides evidence that biallelic *SMARCB1* mutations are solely responsible for tumor genesis in the majority of AT/RT cases. Therefore *SMARCB1* mutations are highly specific for these patients. The examination and identification of *SMARCB1* mutations, especially deletions, was the subject of research in this dissertation. The breakpoints of *SMARCB1* deletions have not yet been identified and mapped extensively. Breakpoint examinations could reveal especially liable regions on chromosome 22, identifying these regions could further allow the prediction of tumor genesis in future. In any case, the understanding of this region is of great interest. The breakpoint identification was successful for patient 2, revealing breakpoints at chromosome 22 positions 3.519.779 and 3.567.270. The mutation mechanism behind the homozygous deletion seems to have been a DNA double stranded break on one allele, followed by an NHEJ-pathway repair mechanism with the loss of 5006 nucleotides. Subsequently, a somatic partial uniparental isodisomy involving this region lead to a biallelic loss of *SMARCB1* integrity. Breakpoints could not be identified for patient 1 and 5, however, the breakpoint regions have been narrowed down to approximately 500 base pairs. These breakpoint regions together with the breakpoints of patient 2 have been compiled in a single map to reveal possible breakpoint accumulations along the chromosome. The sample number is yet too small to propose a significant accumulation.

Close monitoring is indispensable in cancer patients that have gone into remission. Sensitive methods that detect residual tumor cells are therefore required. Since *SMARCB1* mutations are highly specific for AT/RT patients and genetically stable, the mutations are suitable to serve as molecular markers. The cells containing these tumor specific mutations could be detected and quantified using real-time PCR. Therefore, mutation specific primers have been developed for a total of five patients to detect residual tumor cells in peripheral blood and cerebrospinal fluid of the patient. The results were entirely negative for all patients, either because the detection limit, which ranged from 1% - 18% tumor cells in a background of wild type DNA, was not low enough or because the

patients did not have any tumor cells in the blood or CSF respectively. Future research objectives could certainly optimize experimental conditions and achieve higher sensitivities. Nevertheless, there is still a problem with the ambiguity of possible positive results, which is continuously a central challenge in developing methods for minimal residual disease in solid tumors.

6 List of Abbreviations

A-EJ	Alternative end joining
ALL	Acute lymphatic leukemia
ATP	Adenosintriphosphate
AT/RT	Atypical Teratoid Rhabdoid Tumor
B-NHEJ	Backup – Non Homologous End Joining
CNS	central nervous system
Cq	Cycle of Quantification (also known as crossing point/threshold cycle)
CSF	Cerebrospinal fluid
DSB	Double-strand break
dsDNA	double-stranded DNA
EMA	epithelial membrane antigen
ER-MRT	Extra-Renal Malignant Rhabdoid Tumor
FFPE	formalin-fixed paraffin-embedded
GFAP	glial fibrillary acidic protein
HE	hematoxylin and eosin
HR	Homologous recombination
LINES	long interspersed nucleotide elements
MDR	Mini-direct repeat
MEPS	Minimal Efficient Processing Segment
MIR	mammalian-wide interspersed repeat
MLPA	Muliplex Ligand-dependent Probe Amplification
MMEJ	Micro-homology Mediated End Joining
NHEJ	Non-homologous end joining
pBL	peripheral Blood
PCR	Polymerase Chain Reaction
RTK	Rhabdoid Tumor of the Kidney
RTPS	Rhabdoid Tumor Predisposition Syndrome
SINES	short interspersed nucleotide elements
SMA	smooth-muscle actin
SMARCB1	SWI/SNF Matrix Associated Actin-dependent Regulator of

	Chromatin, Subfamily B, Member 1
SNP	Single Nucleotide Polymorphism
ssDNA	single stranded DNA
T_m	Melting Temperature

7 Literature Cited

1. Alberts B, Wilson J, Hunt T. Molecular biology of the cell. 5th ed. New York: Garland Science; 2008.

2. Bednarz-Knoll N, Alix-Panabières C, Pantel K. Clinical relevance and biology of circulating tumor cells. Breast Cancer Res 2011; 13(6):228.

3. Biegel JA, Zhou JY, Rorke LB, Stenstrom C, Wainwright LM, Fogelgren B. Germline and acquired mutations of INI1 in atypical teratoid and rhabdoid tumors. Cancer Res 1999; 59(1):74–9.

4. Bishop JA, Ali SZ. Pediatric Atypical Teratoid/Rhabdoid Tumors: Differential Diagnosis. In: Hayat M, editor. Pediatric Cancer, Volume 2. Dordrecht: Springer Netherlands; 2012. p. 53–8 (Pediatric Cancer).

5. Boboila C, Jankovic M, Yan CT, Wang JH, Wesemann DR, Zhang T et al. Alternative end-joining catalyzes robust IgH locus deletions and translocations in the combined absence of ligase 4 and Ku70. Proceedings of the National Academy of Sciences 2010; 107(7):3034–9.

6. Bourdeaut F, Lequin D, Brugieres L, Reynaud S, Dufour C, Doz F et al. Frequent hSNF5/INI1 Germline Mutations in Patients with Rhabdoid Tumor. Clinical Cancer Research 2011; 17(1):31–8.

7. Burger PC, Yu IT, Tihan T, Friedman HS, Strother DR, Kepner JL et al. Atypical teratoid/rhabdoid tumor of the central nervous system: a highly malignant tumor of infancy and childhood frequently mistaken for medulloblastoma: a Pediatric Oncology Group study. Am J Surg Pathol 1998; 22(9):1083–92.

8. Bustin SA, Benes V, Garson JA, Hellemans J, Huggett J, Kubista M et al. The MIQE Guidelines: Minimum Information for Publication of Quantitative Real-Time PCR Experiments. Clinical Chemistry 2009; 55(4):611–22.

9. Cairns BR, Kim YJ, Sayre MH, Laurent BC, Kornberg RD. A multisubunit complex containing the SWI1/ADR6, SWI2/SNF2, SWI3, SNF5, and SNF6 gene products isolated from yeast. Proc Natl Acad Sci U S A 1994; 91(5):1950–4.

10. Chamberlain JS, Gibbs RA, Ranier JE, Nguyen PN, Caskey CT. Deletion screening of the Duchenne muscular dystrophy locus via multiplex DNA amplification. Nucleic Acids Res 1988; 16(23):11141–56.

11. Chang CH, Housepian EM, Herbert C, JR. An operative staging system and a megavoltage radiotherapeutic technic for cerebellar medulloblastomas. Radiology 1969; 93(6):1351–9.

12. Chi SN, Zimmerman MA, Yao X, Cohen KJ, Burger P, Biegel JA et al. Intensive Multimodality Treatment for Children With Newly Diagnosed CNS Atypical Teratoid Rhabdoid Tumor. Journal of Clinical Oncology 2008; 27(3):385–9.

13. Cote J, Quinn J, Workman JL, Peterson CL. Stimulation of GAL4 derivative binding to nucleosomal DNA by the yeast SWI/SNF complex. Science 1994; 265(5168):53–60.

14. Devita VT. Foreword. In: Pizzo PA, Poplack DG, editors. Principles and practice of pediatric oncology. Philadelphia: Lippincott; 1989 .

15. DKKR / GCCR. Jahresbericht 2011 / Annual Report 2011.

16. Dr. Frank Schakowski. Konzepte und Strategien zur relativen Quantifizierung mit Real-Time-PCR Analysesystemen. Campus Forschung N27, Universitätsklinikum Hamburg Eppendorf, Martinistraße 52, 20246 Hamburg; 2012. (LightCycler Anwendertreffen).

17. Dufour C, Beaugrand A, Le Deley MC, Bourdeaut F, André N, Leblond P et al. Clinicopathologic prognostic factors in childhood atypical teratoid and rhabdoid tumor of the central nervous system. Cancer 2012; 118(15):3812–21.

18. Eaton KW, Tooke LS, Wainwright LM, Judkins AR, Biegel JA. Spectrum of SMARCB1/INI1 mutations in familial and sporadic rhabdoid tumors. Pediatr. Blood Cancer 2011; 56(1):7–15.

19. Flanagan JF, Peterson CL. A role for the yeast SWI/SNF complex in DNA replication. Nucleic Acids Res 1999; 27(9):2022–8.

20. Freireich EJ, Stass SA. Molecular basis of oncology. Cambridge, Mass., USA: Blackwell Science; 1995.

21. Friedberg EC. DNA damage and repair. Nature 2003; 421(6921):436–40.

22. Fruhwald MC, Hasselblatt M, Wirth S, Kohler G, Schneppenheim R, Subero JIM et al. Non-linkage of familial rhabdoid tumors to SMARCB1 implies a second locus for the rhabdoid tumor predisposition syndrome. Pediatr Blood Cancer 2006; 47(3):273–8.

23. Gevertz JL, Dunn SM, Roth CM. Mathematical model of real-time PCR kinetics. Biotechnol. Bioeng. 2005; 92(3):346–55.

24. Ginn KF, Gajjar A. Atypical teratoid rhabdoid tumor: current therapy and future directions. Front Oncol 2012; 2:114.

25. Gordon J.S. Rustin. Chapter 3.4 Circulating Tumor Markers. In: Souhami R, Peckham M, editors. Oxford Textbook of Oncology. 2nd ed.: Oxford University Press; 2002. p. 304 (vol. 1).

26. Gormally E, Caboux E, Vineis P, Hainaut P. Circulating free DNA in plasma or serum as biomarker of carcinogenesis: practical aspects and biological significance. Mutat. Res. 2007; 635(2-3):105–17.

27. Goss PE, Chambers AF. Does tumour dormancy offer a therapeutic target? Nat Rev Cancer 2010; 10(12):871–7.

28. Grabarz A, Barascu A, Guirouilh-Barbat J, Lopez BS. Initiation of DNA double strand break repair: signaling and single-stranded resection dictate the choice between homologous recombination, non-homologous end-joining and alternative end-joining. Am J Cancer Res 2012; 2(3):249–68.

29. Guirouilh-Barbat J, Huck S, Bertrand P, Pirzio L, Desmaze C, Sabatier L et al. Impact of the KU80 pathway on NHEJ-induced genome rearrangements in mammalian cells. Mol Cell 2004; 14(5):611–23.

30. Hasselblatt M, Gesk S, Oyen F, Rossi S, Viscardi E, Giangaspero F et al. Nonsense Mutation and Inactivation of SMARCA4 (BRG1) in an Atypical Teratoid/Rhabdoid Tumor Showing Retained SMARCB1 (INI1) Expression. The American Journal of Surgical Pathology 2011; 35(6):933–5.

31. Hasselblatt M, Isken S, Linge A, Eikmeier K, Jeibmann A, Oyen F et al. High-resolution genomic analysis suggests the absence of recurrent genomic alterations other

than SMARCB1 aberrations in atypical teratoid/rhabdoid tumors. Genes Chromosom. Cancer 2013; 52(2):185–90.

32. Hayat M, editor. Pediatric Cancer, Volume 2. Dordrecht: Springer Netherlands; 2012. (Pediatric Cancer).

33. Holstege FC, Jennings EG, Wyrick JJ, Lee TI, Hengartner CJ, Green MR et al. Dissecting the regulatory circuitry of a eukaryotic genome. Cell 1998; 95(5):717–28.

34. Ichimura K, Nishikawa R, Matsutani M. Molecular markers in pediatric neuro-oncology. Neuro-Oncology 2012; 14(suppl 4):iv90.

35. Joe A., Weinstein I. Oncogene Addiction. In: Schwab M. (Ed.) Encyclopedia of Cancer:: SpringerReference (www.springerreference.com); Springer-Verlag Berlin Heidelberg, 2009 [cited 2013 Mar 25 CET]. Available from: URL:DOI: 10.1007/SpringerReference_175878 2011-01-31 23:00:00 UTC.

36. Kaatsch P, Spix J. German Childhood Cancer Registry - Annual Report 2011 (1980-2010).; 2012 [cited 2013 Mar 4]. Available from: URL:http://www.kinderkrebsregister.de/index.php?eID=tx_nawsecuredl&u=0&file=fileadmin/DKKR/pdf/jb/jb2011/jb2011_kompl.pdf&t=1365081409&hash=96341471b7fe35ca866972ff5e85589d.

37. Kalpana GV, Marmon S, Wang W, Crabtree GR, Goff SP. Binding and stimulation of HIV-1 integrase by a human homolog of yeast transcription factor SNF5. Science 1994; 266(5193):2002–6.

38. Karanam K, Kafri R, Loewer A, Lahav G. Quantitative Live Cell Imaging Reveals a Gradual Shift between DNA Repair Mechanisms and a Maximal Use of HR in Mid S Phase. Molecular Cell 2012; 47(2):320–9.

39. Kieran MW, Roberts CW, Chi SN, Ligon KL, Rich BE, MacConaill LE et al. Absence of oncogenic canonical pathway mutations in aggressive pediatric rhabdoid tumors. Pediatr. Blood Cancer 2012; 59(7):1155–7.

40. Kleihues P, Louis DN, Scheithauer BW, Rorke LB, Reifenberger G, Burger PC et al. The WHO classification of tumors of the nervous system. J Neuropathol Exp Neurol 2002; 61(3):215-25; discussion 226-9.

41. Klochendler-Yeivin A, Picarsky E, Yaniv M. Increased DNA damage sensitivity and apoptosis in cells lacking the Snf5/Ini1 subunit of the SWI/SNF chromatin remodeling complex. Mol Cell Biol 2006; 26(7):2661–74.

42. Krebs JE, Fry CJ, Samuels ML, Peterson CL. Global role for chromatin remodeling enzymes in mitotic gene expression. Cell 2000; 102(5):587–98.

43. Lee D, Sohn H, Kalpana GV, Choe J. Interaction of E1 and hSNF5 proteins stimulates replication of human papillomavirus DNA. Nature 1999; 399(6735):487–91.

44. Lee RS, Roberts CWM. Rhabdoid Tumors: An Initial Clue to the Role of Chromatin Remodeling in Cancer. Brain Pathology 2013; 23(2):200–5.

45. Lee RS, Stewart C, Carter SL, Ambrogio L, Cibulskis K, Sougnez C et al. A remarkably simple genome underlies highly malignant pediatric rhabdoid cancers. J. Clin. Invest. 2012; 122(8):2983–8.

46. Leon SA, Shapiro B, Sklaroff DM, Yaros MJ. Free DNA in the serum of cancer patients and the effect of therapy. Cancer Res 1977; 37(3):646–50.

47. Lieber MR, Ma Y, Pannicke U, Schwarz K. Mechanism and regulation of human non-homologous DNA end-joining. Nat Rev Mol Cell Biol 2003; 4(9):712–20.

48. Liskay RM, Letsou A, Stachelek JL. Homology requirement for efficient gene conversion between duplicated chromosomal sequences in mammalian cells. Genetics 1987; 115(1):161–7.

49. Livak KJ, Flood SJ, Marmaro J, Giusti W, Deetz K. Oligonucleotides with fluorescent dyes at opposite ends provide a quenched probe system useful for detecting PCR product and nucleic acid hybridization. PCR Methods Appl 1995; 4(6):357–62.

50. Livak KJ, Schmittgen TD. Analysis of relative gene expression data using real-time quantitative PCR and the 2(-Delta Delta C(T)) Method. Methods 2001; 25(4):402–8.

51. Loda M, Xu X, Pession A, Vortmeyer A, Giangaspero F. Membranous expression of glucose transporter-1 protein (GLUT-1) in embryonal neoplasms of the central nervous system. Neuropathol Appl Neurobiol 2000; 26(1):91–7.

52. Lopez BS, Corteggiani E, Bertrand-Mercat P, Coppey J. Directional recombination is initiated at a double strand break in human nuclear extracts. Nucleic Acids Res 1992; 20(3):501–6.

53. Louis DN, Ohgaki H, Wiestler OD, Cavenee WK, Burger PC, Jouvet A et al. The 2007 WHO classification of tumours of the central nervous system. Acta Neuropathol. 2007; 114(2):97–109.

54. Michael Frühwald. A multinational registry for rhabdoid tumors of any anatomical site: European Rhabdoid Registry EU-RHAB; 2010.

55. Mukherjee S. The emperor of all maladies: A biography of cancer. 1st ed. New York: Scribner; 2011.

56. Mulcahy HE, Croke DT, Farthing MJG. Cancer and mutant DNA in blood plasma. The Lancet 1996; 348(9028):628.

57. Mülhardt C. Der Experimentator: Molekularbiologie, Genomics. 6th ed. Heidelberg: Spektrum Akad.-Verlag; 2009. (SAV Biowissenschaften).

58. munzinge. Microsoft Word - EURHAB 101115_B.doc.

59. Packer RJ, Biegel JA, Blaney S, Finlay J, Geyer JR, Heideman R et al. Atypical teratoid/rhabdoid tumor of the central nervous system: report on workshop. J Pediatr Hematol Oncol 2002; 24(5):337–42.

60. Pantel K. Detection of minimal disease in patients with solid tumors. J Hematother 1996; 5(4):359–67.

61. Parkinson DR, Dracopoli N, Gumbs Petty B, Compton C, Cristofanilli M, Deisseroth A et al. Considerations in the development of circulating tumor cell technology for clinical use. J Transl Med 2012; 10(1):138.

62. Pizzo PA, Poplack DG, editors. Principles and practice of pediatric oncology. Philadelphia: Lippincott; 1989.

63. Raj GV, Moreno JG, Gomella LG. Utilization of polymerase chain reaction technology in the detection of solid tumors. Cancer 1998; 82(8):1419–42.

64. Roberts CWM, Biegel JA. The role of SMARCB1/INI1 in development of rhabdoid tumor. Cancer Biol Ther 2009; 8(5):412–6.

65. Roberts CWM, Orkin SH. The SWI/SNF complex--chromatin and cancer. Nat Rev Cancer 2004; 4(2):133–42.

66. Rorke LB, Packer RJ, Biegel JA. Central nervous system atypical teratoid/rhabdoid tumors of infancy and childhood: definition of an entity. J Neurosurg 1996; 85(1):56–65.

67. Roth CM. Quantifying gene expression. Curr Issues Mol Biol 2002; 4(3):93–100.

68. Roth DB, Wilson JH. Nonhomologous recombination in mammalian cells: role for short sequence homologies in the joining reaction. Mol Cell Biol 1986; 6(12):4295–304.

69. Rubnitz J, Subramani S. The minimum amount of homology required for homologous recombination in mammalian cells. Mol Cell Biol 1984; 4(11):2253–8.

70. Schneppenheim R, Fruhwald MC, Gesk S, Hasselblatt M, Jeibmann A, Kordes U et al. Germline nonsense mutation and somatic inactivation of SMARCA4/BRG1 in a family with rhabdoid tumor predisposition syndrome. Am J Hum Genet 2010; 86(2):279–84.

71. Serth J, Kuczyk MA, Paeslack U, Lichtinghagen R, Jonas U. Quantitation of DNA extracted after micropreparation of cells from frozen and formalin-fixed tissue sections. Am J Pathol 2000; 156(4):1189–96.

72. Sevenet N, Lellouch-Tubiana A, Schofield D, Hoang-Xuan K, Gessler M, Birnbaum D et al. Spectrum of hSNF5/INI1 somatic mutations in human cancer and genotype-phenotype correlations. Hum Mol Genet 1999; 8(13):2359–68.

73. Sherry L Phillips. Chapter 52 Occupation and Employment Issues in Pediatric Oncology. In: Pizzo PA, Poplack DG, editors. Principles and practice of pediatric oncology. Philadelphia: Lippincott; 1989. p. 1037 .

74. Simsek D, Jasin M. Alternative end-joining is suppressed by the canonical NHEJ component Xrcc4–ligase IV during chromosomal translocation formation. Nat Struct Mol Biol 2010; 17(4):410–6.

75. Smit AF, Hubley R, Green P. Repeat Masker Open-3.0; 1996-2010 [cited 2013 Apr 4]. Available from: URL:http://www.repeatmasker.org.

76. Souhami R, Peckham M, editors. Oxford Textbook of Oncology. 2nd ed.: Oxford University Press; 2002. (vol 1). Available from: URL:http://books.google.de/books?id=CVHTMQEACAAJ.

77. Sudarsanam P, Iyer VR, Brown PO, Winston F. Whole-genome expression analysis of snf/swi mutants of Saccharomyces cerevisiae. Proc Natl Acad Sci U S A 2000; 97(7):3364–9.

78. Takahashi K, Nishihara H, Katoh M, Yoshinaga T, Mahabir R, Kanno H et al. A case of atypical teratoid/rhabdoid tumor in an adult, with long survival. Brain Tumor Pathol 2011; 28(1):71–6.

79. Tekautz TM, Fuller CE, Blaney S, Fouladi M, Broniscer A, Merchant TE et al. Atypical teratoid/rhabdoid tumors (ATRT): improved survival in children 3 years of age and older with radiation therapy and high-dose alkylator-based chemotherapy. J Clin Oncol 2005; 23(7):1491–9.

80. TIB MOLBIOL Syntheselabor GmbH; 2009 [cited 2013 May 2Uhr]. Available from: URL:http://www.tib-molbiol.de/de/oligonucleotides/properties/3-modifications/bhq-1.html.

81. Tsuneyoshi M, Daimaru Y, Hashimoto H, Enjoji M. The existence of rhabdoid cells in specified soft tissue sarcomas. Histopathological, ultrastructural and immunohistochemical evidence. Virchows Arch A Pathol Anat Histopathol 1987; 411(6):509–14.

82. Universite Paris Decartes. Genatlas; 1986 [cited 2013 Apr 5]. Available from: URL:http://www.genatlas.org.

83. Versteege I, Sevenet N, Lange J, Rousseau-Merck MF, Ambros P, Handgretinger R et al. Truncating mutations of hSNF5/INI1 in aggressive paediatric cancer. Nature 1998; 394(6689):203–6.

84. Vogelstein B, Kinzler KW. Cancer genes and the pathways they control. Nat Med 2004; 10(8):789–99.

85. Wang X, Sansam CG, Thom CS, Metzger D, Evans JA, Nguyen PT et al. Oncogenesis Caused by Loss of the SNF5 Tumor Suppressor Is Dependent on Activity

of BRG1, the ATPase of the SWI/SNF Chromatin Remodeling Complex. Cancer Research 2009; 69(20):8094–101.

86. Weinstock DM, Brunet E, Jasin M. Formation of NHEJ-derived reciprocal chromosomal translocations does not require Ku70. Nat Cell Biol 2007; 9(8):978–81.

87. Wilson BG, Roberts CWM. SWI/SNF nucleosome remodellers and cancer. Nat Rev Cancer 2011; 11(7):481–92.

88. Yung E, Sorin M, Pal A, Craig E, Morozov A, Delattre O et al. Inhibition of HIV-1 virion production by a transdominant mutant of integrase interactor 1. Nat Med 2001; 7(8):920–6.

89. Zippelius A, Pantel K. RT-PCR-based detection of occult disseminated tumor cells in peripheral blood and bone marrow of patients with solid tumors. An overview. Ann N Y Acad Sci 2000; 906:110–23.

8 Appendix

8.1 List of Figures

8.2 List of Tables

8.3 Map of Oligonucleotides for Fragment Analysis

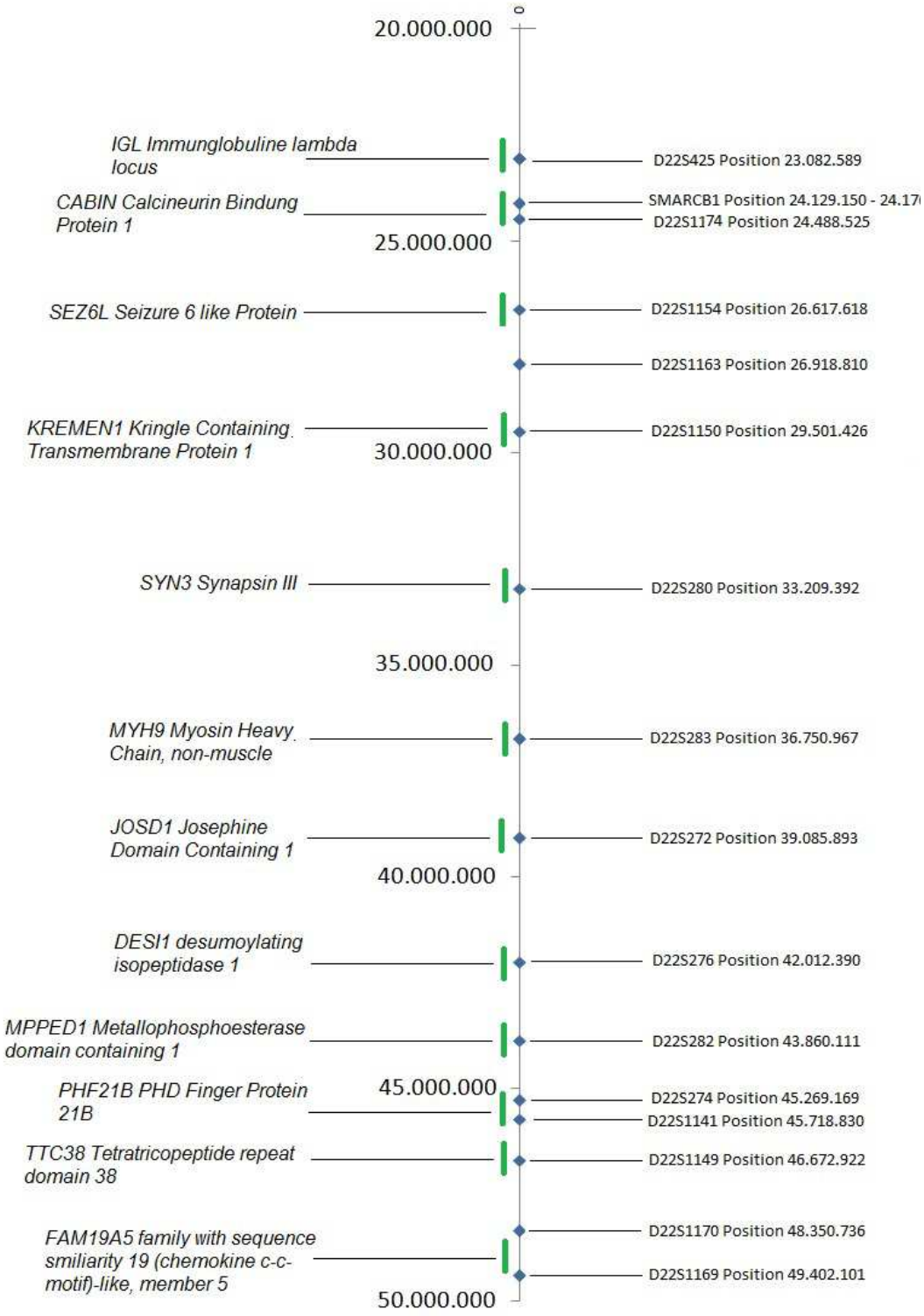

8.4 List of Oligonucleotides for Fragment Analysis

8.5

Name	Position	Forward Primer Sequence 5' - 3'	Reverse Primer Sequence 3' - 5'
D22S686	23.068.521	TTG ATT ACA GAG TGG CTC TGG	TAA GCC CTG TTA GCA CCA CT
D22S425	23.082.589	TGC ACA AGG AGA CAA CTC TG	TCA TGC CCC ATA ACT CAG G
SMARCB1 24.129.150 - 24.176.705			
D22S1174	24.488.525	GAGATCCAGATGTCCATCATTTGG	CAGGGACATAGCAAACTCTTAGG
D22S1154	26.617.618	GGAGCTTCATGTGAATCCCGGC	GTTGACAACATGCACACAGATTGCC
D22S1163	27.918.810	GACTTCAAAGGGAGAGGAAGAAAACC	GCACCGCACTCCAGCCTG
D22S1150	29.501.426	CTACACTTTAAGTAGCAAGGTTCTAGATG	CACCTCAGCTTCATCATCATCTTCC
D22S280	33.209.392	GCT CCA GCC TAT CAG GAT G	GAT TCC AGA TCA CAA AAC TGG T
D22S283	36.750.967	ACC AAC CAG CAT CAT CAT	AGC TCG GGA CTT TCT GAG
D22S272	39.085.893	GAG TTT TGT TTG CCT GGC AC	AAT GCA CGA CCC ACC TAA AG
D22S276	42.012.390	CAT TCT GCC AAG CAA TTT AT	GCT GCT CTT TAA GTT TCT TGA CC
D22S282	43.860.111	TAG GGC TTG CCC AAA GAC	GGC TTG ATG ACA CTG CAT T
D22S274	45.269.169	GTC CAG GAG GTT GAT GC	AGT GCC CAT TTC TCA AAA TA
D22S1141	45.718.830	GTCCCACGTCCTTTAAGGAATAAG	CTCTGCAGCCTCGATGACGG
D22S1149	46.672.922	CCGTCATGAAACCTAATAGTACC	CTTTGCAAGAAGACTGATTCTAGC
D22S1170	48.350.736	GTATTTCAGAGATGATATTTTTATCTC	CATTTTACTTTTGAAGCAAATTCC
D22S1169	49.402.101	CTAATAGCAGAACATGTCTGCAAACTAG	CAGAGGACACCTGCCTGTGG

8.6 List of Oligonucleotidesfor Primer Walking

sorted by patient and position

Name	Position	Forward Primer Sequence 5' - 3'	Position	Reverse Primer Sequence 3' - 5'	Length bp
01_BP1_1	233683	CTT CTG TCT CTC ACA CTT GTT G	234057	CGA TTA CTT CAG GTG AGT TCA C	170
01_BP1_2	233906	CAG CAC AAC ATC GAA GAG GAT T	234057	CTG TCA GGA TGG CAG AGG A	170
01_BP1_3	244118	GGC ATG ATC TTG GCT CAC TG	244265	CAT GAT GAA TCC CCC TCT TTA C	148
01_BP1_4	254308	GAT TGT GGC ATG ACC TAG TC	254468	CCA CAA TGC TTC ACC CCA CA	160
01_BP1_5	263275	CTGGATGCTGTAGTGTCTGGCTCTTC	263275	CAA GGA ATT TCC AAT GCT GTT GGC AAG GC	204
01_BP1_6	273490	CATGGTCTTCCAGACACTGG	273637	AGA GCA CAG ATG ACC ACA CAA	148
01_BP1_6.0.5	274045	GGAAGGGAATTAAATGTGCAGG	274196	CAA GAG AAT CGC TTG AAC CAG	172
01_BP1_6.1	274525	GGCTCATTGCAACCTTTGCC	274660	GAC TGG CCA ACA TGG TGA AAC	136
01_BP1_6.1.5	275028	GTAAAGGGTCCCACATACAAG	275173	CAA GTG AAC TCT CAT AGG GCA G	146
01_BP1_1.2	275701	CATGCTCATTGGGCCATCG	275843	CAG GAA GTG CTA GGT ATG CG	143
01_BP1_6.2.5	276324	GAGTGGCTAGGTTGGAATTTG	276490	GAG AAT CAG CGT GGC AGC C	167
01_BP1_6.3	276597	GTGGACGCCGTTGTCTCTG	276720	CTG CAC AGA AAC CCT GTA G	124
01_BP1_6.3.5	277087	GGAGAATTAAAGGTGGCAGTC	277261	GTC CAG AAC TGT TCC CAG AAC A	175
01_BP1_6.4	277677	GTCTGCTCTTTGTCCTCCTC	277832	CTGTCTCCTTGTGTGATAGTTTC	156
01_BP1_6.4.5	277979	CAGCCAGTGCTGTTCTGAAG	278215	GAA CCC AGG AAC TCT GCA G	237
01_BP1_6.5	278705	GCATATTTCTTCAACCTGGTCATC	278850	CCAGTCTGCTGACACTCTC	146
01_BP1_6.5.5	279316	GCTGCAGTGAGCTGTGTTTG	279450	CAA GGC AGG TAT GCC CTT C	135
01_BP1_6.6	279714	GGTGACCTTTCTTACTTGTCTG	279850	CAG AAT GAG ACT CCT GCA CT	137
01_BP1_6.6.5	280128	GAATCTAGCAGGGTGGTAGG	280291	GCC AAC CTC AGG AAA CTG AAG	164
01_BP1_6.7	280752	GAGATGGAGTTTCGCTCTGTC	280880	CAT GCC TGT AAT CTC AGC TAC	129
01_BP1_6.7.5	281229	CAGCATGTGCTGCATTCGAG	281407	GAG ACA AGA AGA GAA AGA CCA C	179
01_BP1_6.8	281781	GCTCAGTGGCCTGTCATTG	281904	CAG GCC CTG CAT AGC AGC	124
01_BP1_6.8.5	282069	CTAGTAAGTGGAGCCACTCTG	282218	CAG ACT GCT GCA GGC AAA AC	150
01_BP1_6.9	282598	GTGACCACCTCCTTTAATCTG	282717	CTG TGC TCT TGC AGC TCT G	120
01_BP1_6.9.5	293178	CTGCTGCAGCCTCAATCTC	283323	GAC TAG CCT GGG CAA CAT AG	146
01_BP1_7	283738	GTAGAGACTGGGTTTCATCATGTT	283903	GCT AAG TGA AAT AAG CCA GCT G	166
01_BP1_7.5	289192	CTATAACACGTTACTACAAGCTTG	289341	CAC CAT GTT AGC CAG GAT GG	150
01_BP1_8	293838	GTAGAGATGGTGTCTTACTATGTT	293998	GTT TAC AGA TAA GAA AAC AGA AAC C	161
01_BP1_8.5	299114	GACATACCTGTCTGTGGGTAG	299205	CAC AGA GCA CTG AGG AGA AAT G	137
01_BP1_9	303697	GCACATTAAGGTCAAGCAATCAG	303839	CAT GGC CCA TAA CTA ACA GTT C	143
01_BP1_9.5	308223	GCTAGAACTACAACCTGTATGC	308358	CAA CCA CTG CAG CAT CCT C	136
01_BP1_10	313838	CTGAGTACAGAGCTGACCAG	313982	GCA CGC TTC TCA CCA CAC A	145
01_BP1_10.5	319096	CCGTCCTAAGTGCCTGTAG	319249	CCT CAT CAA TGG ACA CTT CTT G	154
01_BP1_11	327152	GGCATTGCCTCCCAGACTG	327329	GAC ATA CAC ACA GGC ACA CTC	177

01_BP1_12	327580	CTCACAGCCCAACTCCAAC	327689	CCA AGT GAG AGA AAC ATG TGA G	110
01_BP2_13	1713092	CTCCTGGCCTCAAGCAATCCTCTTGCC	1713328	CTC TGG CAG TGC AGG GTG AGG TCA C	237
01_BP2_12	1713771	GCCACCCATGTGAGTCCAGCCCAAGG	1713997	GTC CTG AGG AGA GTG TGC AGT AGA TG	227
01_BP2_11	1792218	GCATCTCTTGCTGACCAGAGTGTGGAGTG	1792550	CAC TCC ACA CTC TGG TCA GCA AGA GAT GC	333
01_BP2_10	1892545	CTCCTGCCTCAGCCTCCCAAATAGCTG	1892812	GCC ATG TCT CCT CAG TCC TCT TCA ATA TGG	268
01_BP2_9	1992757	GAGTTGGACTCCTGTATCATCCTCATGCCC	1993051	GCC CAG GAT GGC CTC AAA CTC CTG	295
01_BP2_8	2093010	GGACAAGGCTGATCTCTGCTGTTGGC	2093305	GCA GTC TGA CAA TGT GCC ATT GCT AAG GGC	296
01_BP2_7	2193232	CAGTCCTCCATGGGAACCCTGAACAG	2193501	CTT GGG ATG AGC GGT TGT TGG CTT ATG GC	270
01_BP2_6	2293443	GGTAGGGAGGAATCATGGCATGGCCAG	2293710	GCA TGG TAG CGG GCA CCT GTA GTC C	268
01_BP2_5	2393687	GCCAGGACAGCCCAGGAGTAAAGC	2393952	GAG CAG GTT CCT CCC AGG CCT CTC	266
01_BP2_4	2493920	GACCCCAAGCCAAGCTGCCAGG	2494114	GGT TCC CTT GTA GGG TGA GGG TGA TCT TG	195
01_BP2_3	2594441	GAGACATCATCTCACCCCAGCTAGAGTGA	2594826	GCT GCA GTA AAC GTG GGA GTG CAG G	286
01_BP2_2.9	2604721	CAGTCTGACGATGAGGCTGAGTATCACTG	2604951	GTC ATG GCC TGC ATC TGC TTC TGC C	231
01_BP2_2.8	2613646	CTGTGGTGGGCAGGATGCTCATGAC	2613864	GGA GGC CAC GGA TCC TAC AGG AG	219
01_BP2_2.7	2623665	CTGGTCATCATGTTGCCCGCCTTTCC	2623912	CTT CCT ACA CAT GGT GGA GGT CAC AG	248
01_BP2_2.6	2633923	GTACGCGGCCAGCAGCTATCTGAGC	2634160	GGT TTA TTG AGT GCA GGG AGA AGG GC	238
01_BP2_2.5.8	2635591	GCAGAGAAATGGCCCCTTGGTGCTTG	2635799	GAC AGC TGC TGG GTG TGA AGT AGA CC	209
01_BP2_2.5.7	2636734	CAGCCATCCTTCCAGGGTGAACAATTC	2636957	CCT CTT ATC CTC TGA GTA ATC AGG AGC C	224
01_BP2_2.5.6	2637922	GACCCTTGCTTGCCTCAGCAGGTC	2638151	GTA ACC CAA GGG CAA AGC TGT TCC G	230
01_BP2_2.5.5	2639123	GCCCTCCTCTGAGGAGCTTCAAGCC	2639355	GCG TGA CCT GGC AGC TGT AGC TTC	233
01_BP2_2.5.4.3	2639574	CTCACATATAATTCCTAGCCTTCCCTGG	2639752	CTG GAG GCT CAG GGG TAT GGT GG	179
01_BP2_2.5.4.2	2639838	GTGTCGTCTGTGTCTGGTCATGTGCC	2640027	CAG GGA CCA CTC TGC AGG GAC AAC	190
01_BP2_2.5.4.1	2640032	GCAGTTCTTGCCCACCTGGGAAGG	2640253	GTG ATG GCA CCT AGT AAA TGG TCT CCT AAC	222
01_BP2_2.5.4	2640279	GATTGTGCCATCACCCGGGAGACATG	2640508	GTC CCA GCA CTA GTG ACA TGA ACA CCA G	230
01_BP2_2.5.3	2641298	CTGTCTGGCCCCATTTCATAGATGTGAACG	2641519	GGG TCA ACA TGA GCT GTA TTA TCC TCC TG	222
01_BP2_2.5.2	2642539	GCACATCTTTCTCCTGCCTTGTGCCTGG	2642751	CCA GCC TCA ACC TCC AGG GAG AAG TTG	213
01_BP2_2.5.1	2643136	CGCTTGGTCGACTGTCCCATCTCAGC	2643351	CTA AAA TGA TCA GCT GGG TTC CTC CAC C	216
01_BP2_2.5	2644002	GCAACCTCCTTAAATTCTAAGCAAGGATGAG	2644239	CTC ACT AAG TTG GCT GGG ATG GTG AGC	238
01_BP2_2.4	2654032	GGCCAGACCTGCTTCATGACAGG	2654280	CCA GAC AGG CTT AGA CCT TAG CCT TCG	250
01_BP2_2.3	2664246	GCCCAGAGCGAAGTCACATGTTCAGC	2664463	GAC CCC AGC CAG GTG CTC CCT AC	218
01_BP2_2.2	2674307	GCCTCTGGCTGCTCTGGAGATCTAG	2674554	GCC AGG CTG GGG ACT GAA GAC TTG G	248
01_BP2_2.1	2684563	GCATATGAATGCTGACCACATGGCACATG	2684814	CTC CCA ACG TTG CCA CAA CGG GGA C	252
01_BP2_2	2694624	GCCAGTGGTAAAATATATATGTGGTTAAAGTCTCTG	2694954	GGA TTA CTG GCA TGA GCC ACT GTA CCT G	331
01_BP2_1	2794842	GGACTGGTCATGGCAGGGATGCTGGGC	2790594	GCT GCT GCT GTT GGG GGC AGC TTG GC	253
01_BP3_1	3567153	CCTCCCCAGTCTCTGGGGTCAGG	3567387	GTG TGC CAA CCT TGT TCA CAT ACC	235
01_BP3_1.1	3577281	CTGTGAGTAGGCTTCCAGCTAGCCC	3577511	CCT GGA AAG TCC AGA TTC TGC TAC CAG	231

01_BP3_1.2	3587234	GTCTGGGATGTGAGGAGCGCCTC	3587440	CCT CCC GGA CGG GGT GGC TGC	207
01_BP3_1.3	3597201	GCCTCCCGAGTAGCTGGGATTACAG	3597425	GTG CAC TGA AGT GGG TGC TCA AAT GC	225
01_BP3_1.4	3607441	CCTGACCTTAGGTGATCCACCCACC	3607648	GGC TGG GCA TGG TGG CTC ATG CC	208
01_BP3_1.5	3617479	GGCCTGTTCCTTCCTGAGACCAAAGG	3617711	CTT AAA TGA GGA ATG CAG GAG GGA GTG AG	233
01_BP3_1.6	3627281	GTGCCGGACGGGTTCCTCTCCG	3627513	GCC CGC CCC AGC GAC CTC GTC	233
01_BP3_1.7	3637362	GCATAGTTACTGTGGGTGGGTGTCTGG	3637596	CCA GGC AAT CCC AGG TTT GCC ACA AG	235
01_BP3_1.7.5	3642927	CCAATCAACTCTTCACCCAAGACTCAATC	3643148	GCT GAT AGG AGG CTG ATC AGT AAA CAC TG	222
01_BP3_1.8	3646961	GCGTTTCGCCCCTGCGTTCTCTGAG	3647203	CAT TCC ACA CCC ATC AGG TTG GCA CG	243
01_BP3_1.8.1	3648001	CAGATAATAGCCTTAACCAGAGCCCTGGC	3648269	CTC CCT GTG TGT GCC AGG TTG CTC	269
01_BP3_1.8.2	3649035	GCCTTGGTCCAAGTATGGGTAGCAC	3649268	GGA TTA CAG GCA CAT GCT GCC ACA C	234
01_BP3_1.8.3	3650142	GGACCAGCTCAGCCCGCTATGGATG	3650357	CTC ACC ATG TTG CCC AGG CTG GTC	216
01_BP3_1.8.4	3651394	GCAGTGGCTCACCCTTGTTTCGGC	3651656	GCT GCC AGA GCC TTG GGT ATT CAG	263
01_BP3_1.8.5.1	3651726	GCGATTGGCCTTAGACTATTTACTAGC	3651901	CTG GTC TTG AAC TCC TGA CCT CAA G	176
01_BP3_1.8.5.2	3651964	GGTGCACGCCTGTAGTCCCAGC	3652096	GGGTGACAGAGCGAGACTCTGTCTC	133
01_BP3_1.8.5.3	3652283	CTGTGGTCCCAGCTACTAGGGAG	3652406	GAG ATG AGT CAC GCT CTG TCG CC	124
01_BP3_1.8.5	3652561	GGCCTCTAGTGGCCTCTGTTCTGTTAC	3652764	CTT CAT GCT GAC AGG GAA CAG TGA GGC	204
01_BP3_1.8.6	3653847	CTAAGCAGGCCAGGCGTAGTGGCTC	3654047	CTC CTG CCT CAG CCT CCT GAG TAG C	201
01_BP3_1.8.7	3655140	CTCATGCCAATTGAATCCTGTGGCAGC	3655348	GGT TTG GTT AAT AGG ACC TGT TCA TAG GTC	209
01_BP3_1.8.8	3656405	CTTGGCTCACTGCAACCTCCACCTC	3656601	CAT TTT GGG AGG CTG AGG TGG GCA G	197
01_BP3_1.8.9	3657250	GGAGGCTCACACCTGTAATCCCAGC	3657467	CTC TTT GCA ACC TCC ACC TCC CAC G	218
01_BP3_2	2667414	GATGGGAGACTCACTTAAGGCCAGCAC	3667641	GAG ACA GGG TCT CGC TCT GTC ACC	228
01_BP3_3	3767701	CTCTCTCGCCCAGGCTGGAGTGC	3767927	GAG GCG GAG GCA GGC AGA TCA C	227
01_BP3_4	3868276	CCAGGTGCAGTGGCTCACGCCTG	3868524	GAG TGC AGT GGA ACA ATC TCG GCT CAC	249
01_BP3_5	3968374	GACCAGCAGAGGCCTCCGCCTG	3968604	GAG GAG GCC GAG AGA TGC TTG CAA G	231
01_BP3_6	4068466	CAGAGCCTGCTGGGTGGGAGAC	4068711	GGA TCA GCT GGC ACC ATC CAG ATC G	246
01_BP3_7	4169008	GAGAGGCCGAGGCAGGCGGATC	4169244	GGA GTC TTG CTC TGT TGC CCA GGC	237
01_BP3_8	4269472	CCAGATAGACTAGCTACTCTGCAATGGC	4269728	GGT CCA GAG GTG GGA TAA ACA GTA GCT G	257
01_BP3_9	4344362	GTGAGGCTGTGTGGGAGGAATGGCC	4344638	CTG AAG GAA GTA GCA CTT CTC CCA AAT AG	277
Name	Position	Forward Primer Sequence 5' - 3'	Position	Reverse Primer Sequence 3' - 5'	Length bp
02_BP1_1	2828310	GCTGCAGTGTGGCTCGGCCTCAC	2828483	CTC TGA GCT TTG CCG ACA TCC CAT GG	174
02_BP1_2	2828543	GCGGCAACGCCGCGAAATCAAGC	2828714	GAT GAT GCG GGT CAG CGA GTC GAT G	172
02_BP1_3	2838765	GGAGCTCCAGGCCCTTTCGGAGC	2838946	CTC TGT ATT CCC AAG GGT GTT GGT CAA AG	182
02_BP1_4	2848957	GCTGCCAGGTGAGGGGCTGAGG	2849129	CTC ACT GCA CTT CTG GGC CCC TCA G	173
02_BP1_5	2859141	CTCCTCCTGAGCCTGCCTTGTTCCG	2859314	GAG TTT CCA ACA CCC CTT CCC ACT CG	174

02_BP1_6	2869114	CAACCTGGGCAGTTCAGGGCAGCTAC	2869317	CAT TAG CAA GGC AGG AAG ACA TGG TGA AG	204
02_BP1_7	2879161	GACTGAGGTTTCACTTTGTTGCCCAGGC	2879356	CCA GGA GAA AGA CAG TTA AGG AGC TGT GC	196
02_BP1_8	2979366	GGTGCAGCTGGGCACAGTCAAGC	2979597	CTT CAG GGA GGT AAG TTC CTC TGA CAG C	232
02_BP1_9	3080217	GCTGCACCTATTGACCCATCCTCTAAG	3080423	GTC CTC TGG AGG GAC ATG GAT GAA GC	207
02_BP1_10	3180358	GTTCGGAGACACAGTTCAGGTACTTGG	3180558	CTG GAG CAG TGC CTG TCT CCG GC	201
02_BP1_11	3280199	GGTCTCCTGCAGTACCCTCAGGCTTAC	3280412	CAG AAG GCA GAG CAA AGA TGA CAT GCT TC	214
02_BP1_12	3380920	CTGAGTTCAAGCGACTCTCCTGCCTC	3381120	GGA GAA TCA TTT GAA CCC CAG AGG TGG	201
02_BP1_12.1	3391113	CGGCTTCCCAAAGTGCTGGGATAACAGG	3391268	GAG GTT GCG GTG AGG GAA GAT CGC AC	156
02_BP1_12.2	3400457	GAGGCATCACGCTACCTGACTTCAAAC	3400608	GTC AAA GAT CAG ATA GTT GTA GGT ATG CGG C	152
02_BP1_12.3	3410667	GACCTCCTACCACCAGGGCAGCC	3410831	GAC CTG TGA TTG GGA GTC TCC AGG TGA G	165
02_BP1_12.4	3420896	GCTCACTTCGTAGGCGATGCTCGAGAG	3421054	GGC AAA GGG CCA GAG GCG TCG AG	159
02_BP1_12.5	3431080	GCTCAGTGACAAAGAGAGGTGAGGGC	3431232	GAG CCC AGA AGG CAG ACG TTG CAG	153
02_BP1_12.6	3441183	GGTGGCAGGAAATTGACTCACAGGTGAC	3441348	CCT GCA AGT CTA CAC TGA TCA TTG CCT TC	166
02_BP1_12.7	3450842	GCAATGAGCCGAGGTTACACCACTGC	3450985	CCA CAC GGT GCC TTC CCT ACT GGA G	144
02_BP1_12.8	3460801	GTGCCAGACCCTCATCTGGGGTCTC	3460972	CTA GTA CAG CCT GCA GAA CCA TGA GC	172
02_BP1_12.9	3471133	GATGGAGTCTTGCTCTGTCACCCAGGC	3471276	GCT GGG CAT GGT GGT TTG TGC CTG TAA TC	144
02_BP1_12.10	3481081	GCAGCCTTGACCTCCCCGGCTC	3481238	GAG CCC AGG AGT TCA AGA CCA GCC	158
02_BP1_12.11	3491047	GCTCAAGTGATCCTCCCACCTCAGG	3491191	CAA GAC CAG CCT GGG CAA CAT AGT AAG	145
02_BP1_12.12	3501121	GTCTGTCCCCTCCCTCCAGACAG	3501276	CAA CAG TCG AAG ACG GGT TGG GAC G	156
02_BP1_12.12.1	3503355	GCACACCGGTAGTCCCAGCTACTTGG	3503465	GAG ACA GGG TCT TGC TCA ATG GTG TGA TC	111
02_BP1_12.12.2	3505730	GGCTCTGCCGCCGGTGAGTGCC	3505874	AGA AAG CGT TTC GGG TAC CGG GCG C	145
02_BP1_12.12.3	3507917	GCCCTGGAGGTGGGAGGCATGAG	3508034	CCA TTT CCC AGA GGA TGA GAC AGA GC	118
02_BP1_12.12.4	3509949	GGCCGAGGCAGGTGGATCATGAGG	3510059	GCA CCC AGC CTC ACG CCT GGC	111
02_BP1_12.12.5	3511682	GGCCTAAGTAGCTGGAGTAGGTGACAGG	3511818	GGC ACC GGC ACA TGG CAG GGC	137
02_BP1_12.12.6	3514086	GCATTGGCCTCTCGCCACTGGCAG	3514229	CCA TAA CAT TCC TGG CTC TGG GAA GTC TC	144
02_BP1_12.12.6.1	3514704	GTCACAGCCAAATGCCAGTGGAAGGAG	3514853	CTG CTC AGC ACC CCA CCC GCA G	150
02_BP1_12.12.6.2	3514943	GGCAGTGGTGGCTGGGCAGGTC	3515083	GGC AGC ATG GAC CGG GAA CCT CAC	141
02_BP1_12.12.6.3	3515345	GGCTCTTCATCACAGGTCCTTTGTCC	3515467	CCA GGG TAA GAC CTT GCA CTT CTC TG	123
02_BP1_12.12.6.4	3515784	GCTATCCTAGGGTAGCCTCCAGCTCC	3515931	GCC TCA GAG GCC TGA GTC CCA CC	148
02_BP1_12.12.7	3516288	CTGCCAACACTTTCCTCTGACCATGGC	3516406	CAT GCC TGG TGC CCA CAG CCA CAA AG	119
02_BP1_12.12.8	3518494	GCTGCAGTGCAGTGGTGCAATCAGC	3518611	GGT GTG GCA TGG CGG TGT GCA C	118
02_BP1_13	3519205	GGAGAAGGTGGAAGGTGTCTCTCCC	3519404	CGC AGT GCA GCT GAG CAG ATA GGC	200
02_BP1_14	3519519	CTGGGCTCAGTTCCAGTCCTGGCTG	3519701	CAA ACA AAA GGC CGG GCG CGC CTC	183
02_BP2_1	3519986	GCTGGAGGACGACGGCGAGTTC	3520180	CGA CAC GCC CAC TAG GCC ACG	198
02_BP2_1.1	3520294	GCTGGGTTGGTTTCCAGTCAGACGC	3520439	GTT CCC ACA AGT AGC AAT ACG GGG AG	146
02_BP2_1.2	3520829	GTCTGGCTATGTTGCGCAGGCAGG	3521002	CTA GCT GGG GAC TGC CTT TGG AGC	174

02_BP2_2	3521216	CTTTGTGCAGTGGTGTGATCTCGGCTC	3521426	GAG GCT GAG GTG CAA GGA TCA CTT GAG	211
02_BP2_3	3521881	CGATTATAGGCGTGAGCCACTGTGCC	3522087	GCA TTC TGC AGT TAG GCA GGT GCC TAC	207
02_BP2_4	3523083	GCGAGTGACTTGCTGTGTCTGCTCTTC	3523291	GAC AAG AGT CTC ACT ATG TTG CCC AGG C	209
02_BP2_5	35242405	CTGGGGGCCACCTCAAGGCCTG	3524605	CCT CTC TTC CAC AGT GGC TAG TCG C	201
02_BP2_6	3524730	CTCCAGAGTGTCTTCACTGCAGCCTTG	3524928	CCA ACA TGT CTT CAC AGC ACC TGC TAG	199
02_Probe	3515691	CAGGGGGCTAGAGCATTTTG	3515889	CAC TTT GGG AGA CCC AGA C	199
Name	Position	Forward Primer Sequence 5' - 3'	Position	Reverse Primer Sequence 3' - 5'	Length bp
03_Probe_1	3536097	CCCGAGGTGCTGGGGAG	3536308	GTC AGG TCC AGA ATC TGC C	64
03_Probe_2	3536130	GGCTGGACATGGAGGCTG	3536308	GTC AGG TCC AGA ATC TGC C	179
03_Probe_3	3536021	CGCTGACTGTTGCTTCCATTTC	3536160	CGA TCT CCA TGT CCA GCC TC	140
Name	Position	Forward Primer Sequence 5' - 3'	Position	Reverse Primer Sequence 3' - 5'	Length bp
04_Probe_1	3549608	CGCCTCTGCCATCAGAGC	3549771	CTT GGT GTA CCC TCA GTG C	164
04_Probe_2	3549482	GCATGGTGCAATCTCTTGGC	3549640	GGT AGG ACT CGA TCT GCT C	159
Name	Position	Forward Primer Sequence 5' - 3'	Position	Reverse Primer Sequence 3' - 5'	Length bp
05_BP1_0	1440151	GGAGGGGTTGGGCCTACACCGG	1440267	CTC TGC TGC TCG CTT CCT GGG AAG	117
05_BP1_1.0	1440268	GAAGAGCCCTCAACCAGTGCCACTG	1440448	GCT GGC AGC AGA GGG CAG GCT AG	181
05_BP1_1.1	1450598	GCTGAGGCAGGAGGATTGCTTGAGCTC	1450780	CCT GAC CTC AGG TGA TCC ACC CAC	183
05_BP1_1.2	1460462	GAGATGGAATCTCTGTCGCCCAGGC	1460675	CAC TCC AGC CTG GGC AAT AAG AGC G	214
05_BP1_1.3	1470352	GCTGGGATTACAGGTGTGAGCCACTG	1470540	CTT TTG CTG TCT CCG TGT GAG GAT TCC	189
05_BP1_1.4	1481267	GTCCCCAGAATGCGGTCGTCCG	1481453	GCG TCG GGA GCA CTA CCC AGA G	187
05_BP1_1	14913632	CCGGTTCCATCTTCCAGATCCCACTG	1491635	GCC AGG CAT GGT GGC ACA CAC CTA T	274
05_BP1_13a	1712792	GTACCTGTTCAGGTGGGCAGATACGC	1712937	GTG TGA GAA GTA GGG GCT CAG GTG C	146
01_BP2_13	1713092	CTCCTGGCCTCAAGCAATCCTCTTGCC	1713328	CTC TGG CAG TGC AGG GTG AGG TCA C	237
05_BP2_13b	1713438	GGTACAGCCGTCCACACTTCTGCC	1713572	GCT GCA GGC CAA GGT TCC TTG CC	135
01_BP2_12	1713771	GCCACCCATGTGAGTCCAGCCCAAGG	1713997	GTC CTG AGG AGA GTG TGC AGT AGA TG	227
01_BP3_1	3567153	CCTCCCCAGTCTCTGGGGTCAGG	3567387	GTG TGC CAA CCT TGT TCA CAT ACC	235
01_BP3_1.1	3577281	CTGTGAGTAGGCTTCCAGCTAGCCC	3577511	CCT GGA AAG TCC AGA TTC TGC TAC CAG	231
01_BP3_1.2	3578234	GTCTGGGATGTGAGGAGCGCCTC	3587440	CCT CCC GGA CGG GGT GGC TGC	207
01_BP3_1.3	3597201	GCCTCCCGAGTAGCTGGGATTACAG	3597425	GTG CAC TGA AGT GGG TGC TCA AAT GC	225

01_BP3_1.4	3607441	CCTGACCTTAGGTGATCCACCCACC	3607648	GGC TGG GCA TGG TGG CTC ATG CC	208
01_BP3_1.5	3617479	GGCCTGTTCCTTCCTGAGACCAAAGG	3617711	CTT AAA TGA GGA ATG CAG GAG GGA GTG AG	233
05_BP2_1	3618733	GGCACCCACATGCCCATTTGCTATCAG	3618890	CTG GAG CCA AGC CAG ACA CAA ATG TGT AC	158
05_BP2_2	3619829	GTTCTCTGTCGCCCAGGCTGGAGG	3619963	GCA GGG CAT GGT GGC TCA CGC C	135
05_BP2_3	3620991	GGCAGGACTGCAGTGGCACTATCTC	362119	GCC AGG CTA GCC GGG CGC G	129
05_BP2_4	3622152	GCCGGAATTGGCTCTGGCCACTCTG	3622291	CCT CTC TGC ACT GCC CTT CCT TGT C	140
05_BP2_5	3623184	GGTACCTGAGGTCCGTGGCGCG	3623344	CCA CTG CTA ATC CAC AGG GTC ACT CTG	161
05_BP2_6	3624481	CTGTCCCCACTGGGATGGAGTTTACC	3624651	CTC ATC CTT CAG TTC TTG GCT CAG CC	171
05_BP2_7	3625570	GCGAGGCTGCACCTTGTCATTCAGG	3625717	CCA GCC CCA GGC AGC AGA GTT AGC	148
05_BP2_8	3626774	GCTCAGTGCGTGCAGTGGAATGAACTG	3626901	CAC TAA GTC ACC GAT GTT AGT CGC CAG	128
01_BP3_1.6	3627281	GTGCCGGACGGGTTCCTCTCCG	3627513	GCC CGC CCC AGC GAC CTC GTC	233
01_BP3_1.7	3637362	GCATAGTTACTGTGGGTGGGTGTCTGG	3637596	CCA GGC AAT CCC AGG TTT GCC ACA AG	235
01_BP3_1.7.5	364297	CCAATCAACTCTTCACCCAAGACTCAATC	3643148	GCT GAT AGG AGG CTG ATC AGT AAA CAC TG	222
01_BP3_1.8	3646961	GCGTTTCGCCCCTGCGTTCTCTGAG	3647202	CAT TCC ACA CCC ATC AGG TTG GCA CG	242
01_BP3_1.9	3657250	GGAGGCTCACACCTGTAATCCCAGC	3657467	CTC TTT GCA ACC TCC ACC TCC CAC G	218
01_BP3_2	3667414	GATGGGAGACTCACTTAAGGCCAGCAC	3667642	GAG ACA GGG TCT CGC TCT GTC ACC	229
01_BP3_3	3767701	CTCTCTCGCCCAGGCTGGAGTGC	3767927	GAG GCG GAG GCA GGC AGA TCA C	227
01_BP3_4	3868276	CCAGGTGCAGTGGCTCACGCCTG	3868524	GAG TGC AGT GGA ACA ATC TCG GCT CAC	249
01_BP3_5	3968374	GACCAGCAGAGGCCTCCGCCTG	3968602	GAG GAG GCC GAG AGA TGC TTG CAA G	229
01_BP3_6	4068466	CAGAGCCTGCTGGGTGGGAGAC	4068711	GGA TCA GCT GGC ACC ATC CAG ATC G	246
01_BP3_7	4169008	GAGAGGCCGAGGCAGGCGGATC	4169244	GGA GTC TTG CTC TGT TGC CCA GGC	237
01_BP3_8	4269472	CCAGATAGACTAGCTACTCTGCAATGGC	4269728	GGT CCA GAG GTG GGA TAA ACA GTA GCT G	257
Name	Position	Forward Primer Sequence 5' - 3'	Position	Reverse Primer Sequence 3' - 5'	Length bp
06_Probe	3536122	TGGACATGGAGATCTCAGCC	3536322	GTC CAG AAT CTG CCT GAC AG	201
06_Probe	3536171	TGGAGATCGATGGGCAGAAGCTGCG	3536495		25
Name	Position	Forward Primer Sequence 5' - 3'	Position	Reverse Primer Sequence 3' - 5'	Length bp
07_Probe_1	3526248	CCACTTGGCTGGCTGCTG	356427	CTG TGC TGA TGG ACA CAC AG	180
	3526328	GACTCTAGCCACCAGTGTGACCCTG	3526352		25
07_Probe_2	3526397	GAAGTACAAGGCTGTGTgtC	3526578	GAC AAG AAC AAG ATT CCA TCT C	182

8.7 List of Instruments and Materials

Instrument / Material	Type	Manufacturer	Location
AgarosegelAgarose	1,2% (v/v)	Invitrogen	Karlsruhe
Purificationof SEQ-Reaction	DyeEx 96 Kit	Qiagen	Hilden
Caps	8er Domed Cap Strips	peqlab	Erlangen
DestilledWater	Aqua ad iniectabilia	Braun	Melsungen
DMSO	DMSO 1 ml	Agilent	Böblingen
DNA Extraction	QiAmp DNA Mini Kit Tissue + Blood + Blood Spot Protocol	Qiagen	Hilden
DNA Size Standard	DNA ladder 100 bp	Invitrogen	Karlsruhe
DNA Size Standard	Gene Ruler Mix	Thermo Scientific	
DNA Quantification Instrument	Qubit® 2.0 Fluorometer	Invitrogen	Karlsruhe
DNA QuantificationTubes	Qubit Assay Tubes	Invitrogen	Karlsruhe
DNA QuantificationReagent	dsDNA Broad Range Reagent 200x with DMSO	Invitrogen	Karlsruhe
DNA QuantificationBuffer	dsDNABroad Range Buffer	Invitrogen	Karlsruhe
DNA QuantificationStandards	dsDNA Broad Range Standard # 1 and # 2	Invitrogen	Karlsruhe
Migrationchamber with mounting plate and microtitier-comb	PerfectBlue Breitformat-Gelsystem Maxi ExW	Peqlab	Erlangen
Ethidiumbromid	0,1 µl/ml		
Fragment Analysis	Hi-Di Formamide	Applied Biosystems	Foster City, USA
Fragment Analysis	Gene Scan 500 LIZ Size Standard	Applied Biosystems	Foster City, USA
Gel Extraction	Ultrafree-DA	Millipore	Bedford, USA
Gel Extraction	QiaQuickGelExtraction Kit for Sequencing	Qiagen	Hilden
Gel Extraction	MinElute Gel Extraction Kit	Qiagen	Hilden
Gel-Documentationssystem	E-Box VX2	Peqlab	Erlangen
LoadingBuffer	Gel-LoadingBuffer III	MBI Fermantas	St. Leon-Rot
Magnesium	25 mM MgCl2	Qiagen	Hilden
MLPA Chromosome 22 DiGeorge	SALSA MLPA kit P250 DiGeorge	MRC-Holland	Amsterdam, NL
MLPA Chromosome 22 *SMARCB1*	SALSA MLPA kit P258 *SMARCB1*	MRC-Holland	Amsterdam, NL
PCR	GoTaq Green PCR Master Mix	Promega	Madison, USA
PCR	DreamTaq Green PCR Master Mix	Thermo Scientific	Waltham, Massachussetts, USA
PCR	ExpandLongRangedNTPack Version 06	Roche	Mannheim

PCR, Fragment Analysis	Taq DNA Polymerase recombinant	Invitrogen	Karlsruhe
PCR, Real-Time Capillary Centrifuge	LC CarouselCentrifuge	Roche	Mannheim
PCR, Real-Time Instrument	Light Cycler I 32-Capillary Carousel-Based System	Roche	Mannheim
PCR, Real-Time LightCycler	QuantifastSYBRGreen PCR Kit	Qiagen	Hilden
PCR, Real-Time LightCycler with Probe	FastStart DNA MasterPlus Hyprobe	Roche	Mannheim
PCR, Real-Time Reaction Vessels	Light CyclerCapillaries (20 µl)	Roche	Mannheim
PCR, Real-Time Instrument II	Light Cycler 480 Instrument II, 96-well block	Roche	Mannheim
PCR, Real-Time Reaction Plates	Light Cycler 480 Multiwell Plate 96	Roche	Mannheim
PCR, Real-Time	Light Cycler 480 SealingFoil	Roche	Mannheim
PCR, Real-Time CFTR-Gene			
Pipettes	Pipetman	Gilson	Middleton, USA
Pipetten Filtertips	BiosphereFiltertips 10µl, 100 µl, 200 µl, 1250 µl type Eppendorf/Gilson	Sarstedt	Nümbrecht
SEQ Buffer	5xSequencing Buffer	Applied Biosytsems	Foster City, USA
SEQ Kit	ABI Prism BIG DYE Termi-nator Cycle Vers. 3.1	Applied Biosytsems	Foster City, USA
SEQ-Tubes	Softtubes 0,5 ml	Biozym, Hess. Oldendorf	NA
Sequencer	ABI-Prism 3130 Genetic Analyzer	Applied Biosystems	Foster City, USA
Power source	Desatronic 3000/200	Desaga	Heidelberg
Thermo Fast 96 PCR Plates	0,2 ml Tube Plate	peqlab	Erlangen
Thermocycler	T-Gradient	Biometra	Göttingen
Thermocycler	T1-Thermocycler	Biometra	Göttingen
Tris-Acetat-EDTA-Buffer	1x	Millipore	Bedford, USA
UV-Light table	ECX-20M	Peqlab	Erlangen
Vortex	Certomat MV	B.BraunBiotech	
Centrifuge 96 Multiwel Plates	Heraeus Multifuge 3 S-R	Thermo Scientific	
Centrifuge 1,5 ml Tubes	EBA 12R	Hettich-Zentrifugen	Tuttlingen
Whole Genome Replication	Repli-G Mini Kit	Qiagen	Hilden

8.8 List of Softwares

Program	Manufacturer
Adobe Photoshop CS3 Vers. 10.0	Adobe Systems Incorporated
BLAST Basic Local Alignment Search Tool	Nationel Center for Biotechnology Information, Bethesda, USA
Genatlas	Université Paris Decartes
Lasergene 8 SeqBuilder Vers. 8.0.3 (1)	DNASTAR
Light Cycler Program Data Analysis 3.5.28	Roche Applied Science, Idaho Technology Inc. 1998
Light Cycler Program Front Version 3.5	Roche Applied Science, Idaho Technology Inc. 1998
Light CyclerProgramGraphworks 10.0.7	Roche Applied Science, Idaho Technology Inc. 1998
Light Cycler Program Run Version 5.32	Roche Applied Science, Idaho Technology Inc. 1998
Light Cycler 480 Software release 1.5.0 SP4	Roche Applied Science, Idaho Technology Inc. 1998
Map Viewer	Nationel Center for Biotechnology Information, Bethesda, USA
Microsoft Paint	Microsoft
Office Excel 2007	Microsoft
OligoCalculator	Metabion international AG, Martinsried
RepeatMasker	http://www.repeatmasker.org
SeqPilot	JSI Medical Systems, Kippenheim, Germany

9 Acknowledgments

This dissertation was one of the first hands-on experiences in the field of scientific research for me. It has been a very rewarding experience.

First and foremost, I would like to express my deepest gratitude to Professor Dr. rer. nat. Reinhard Schneppenheim for offering me this compelling thesis, for sharing his ideas and for his sincere encouragement and advice. I thank him for the opportunities to attend the Rhabdoid-Congress 2013 in Paris, France and the 27th Annual meeting for the Kind-Philipp-Foundation for Leukemia Research 2014 in Wilsede, Germany as presenting author. I also thank him for allowing me to be first-author on the paper published in Cancer Genetics “Identifying Molecular Markers for the sensitive Detection of Residual Atypical Teratoid Rhabdoid Tumor Cells” and his support during the entire review process.

Furthermore, I express my most genuine gratitude to Florian Oyen and Tobias Obser for their excellent supervision, unflagging support and assistance.

I also want to thank Cordula Steglich, Susanne Heinsohn and Dr. Udo zur Stadt for their patient and generous instructions on the Light Cycler Instruments.

And finally, I thank my family for their everlasting love and their support throughout my studies.

10 Statutory Declaration

Ich versichere ausdrücklich, dass ich die Arbeit selbständig und ohne fremde Hilfe verfasst, andere als die von mir angegebenen Quellen und Hilfsmittel nicht benutzt und die aus den benutzten Werken wörtlich oder inhaltlich entnommenen Stellen einzeln nach Ausgabe (Auflage und Jahr des Erscheinens), Band und Seite des benutzten Werkes kenntlich gemacht habe.

Ferner versichere ich, dass ich die Dissertation bisher nicht einem Fachvertreter an einer anderen Hochschule zur Überprüfung vorgelegt oder mich anderweitig um Zulassung zur Promotion beworben habe.

Ich erkläre mich einverstanden, dass meine Dissertation vom Dekanat der Medizinischen Fakultät mit einer gängigen Software zur Erkennung von Plagiaten überprüft werden kann.

Unterschrift: .....